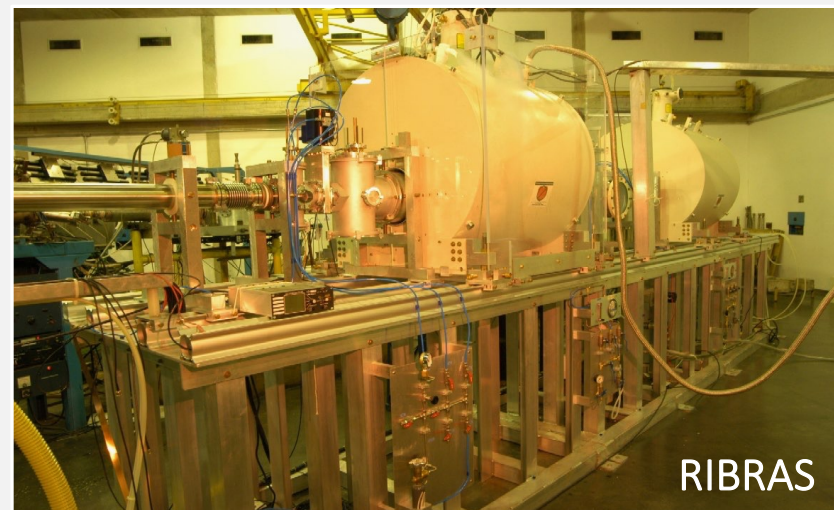
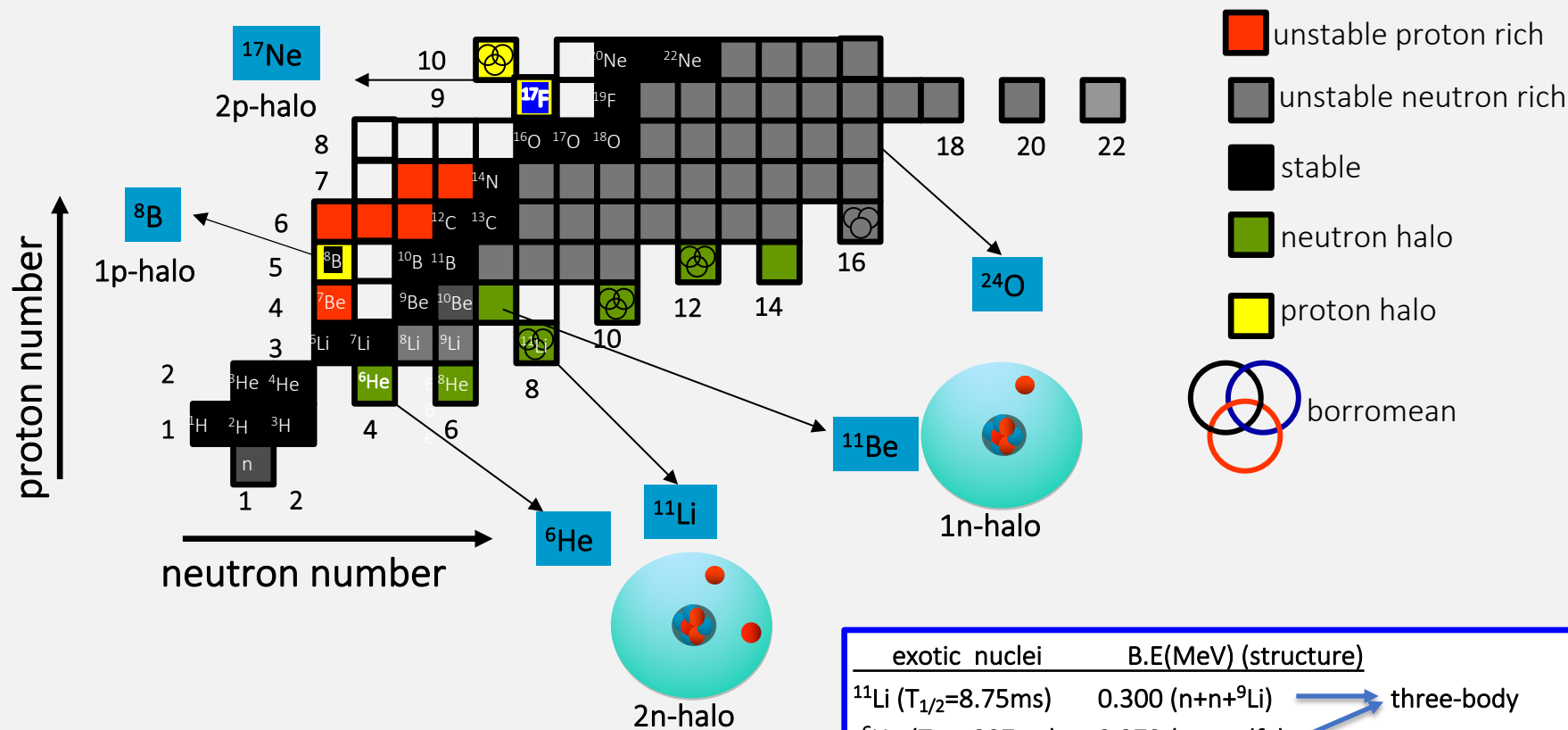


# Inclusive breakup reactions in low energy unstable nuclei collisions

- Introduction: light exotic nuclei
- Inclusive breakup reactions induced by  $^8\text{Li}$
- Inclusive breakup reactions induced by  $^6\text{He}$
- Comparison with more exotic projectiles  $^{11}\text{Li}$ ,  $^{11}\text{Be}$  and  $^8\text{B}$
- Conclusions



light weakly bound nuclei – Clusters and Halos



binding energies of ‘normal’ nuclei 7-10 MeV

weakly bound nuclei	B.E(MeV) (structure)
$^6\text{Li}$	1.47 ( $\alpha$ +d)
$^7\text{Li}$	2.46 ( $\alpha$ +t)
$^9\text{Be}$	1.67 ( $\alpha$ + $\alpha$ +n)
$^8\text{Li}$	2.03 ( $^7\text{Li}$ + n)

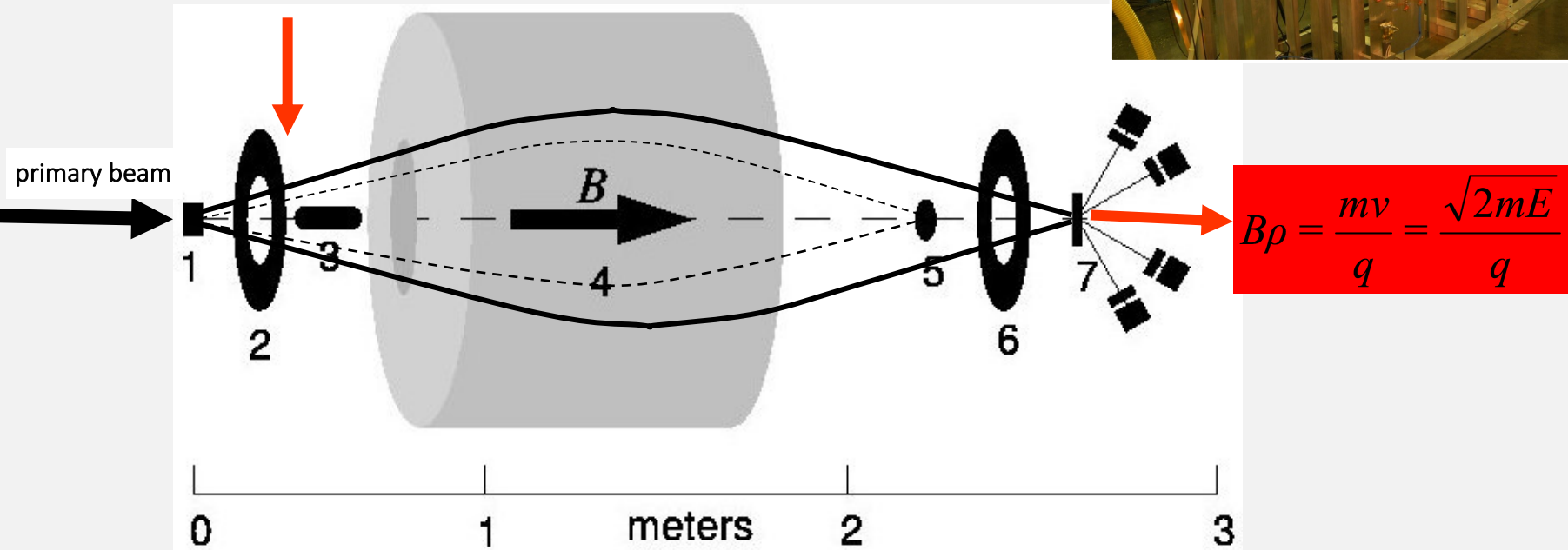
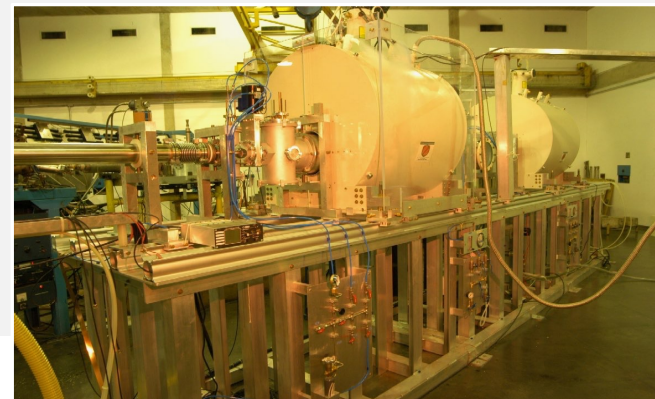
exotic nuclei	B.E(MeV) (structure)	
$^{11}\text{Li}$ ( $T_{1/2}$ =8.75ms)	0.300 (n+n+ $^9\text{Li}$ )	three-body
$^6\text{He}$ ( $T_{1/2}$ =807ms)	0.973 (n+n+ $\alpha$ )	
$^{11}\text{Be}$ ( $T_{1/2}$ =13.81s)	0.501 (n+ $^{10}\text{Be}$ )	
$^8\text{B}$ ( $T_{1/2}$ =770 ms)	0.137 (p+ $^7\text{Be}$ )	
$^{17}\text{F}$ ( 64.5 s)	0.6 MeV (p+ $^{16}\text{O}$ )	
	0.1 MeV for 1st $^{17}\text{F}$ excited state	

- The RIBRAS system: secondary beam selection

First solenoid

angular acceptance  
 $2 \text{ deg} < \Delta\theta < 6 \text{ deg}$

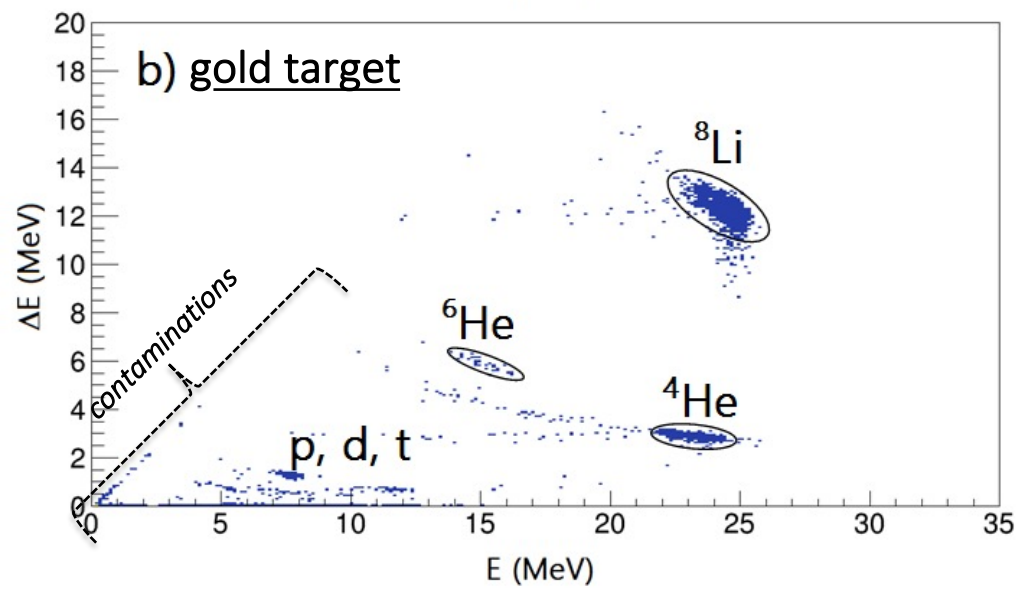
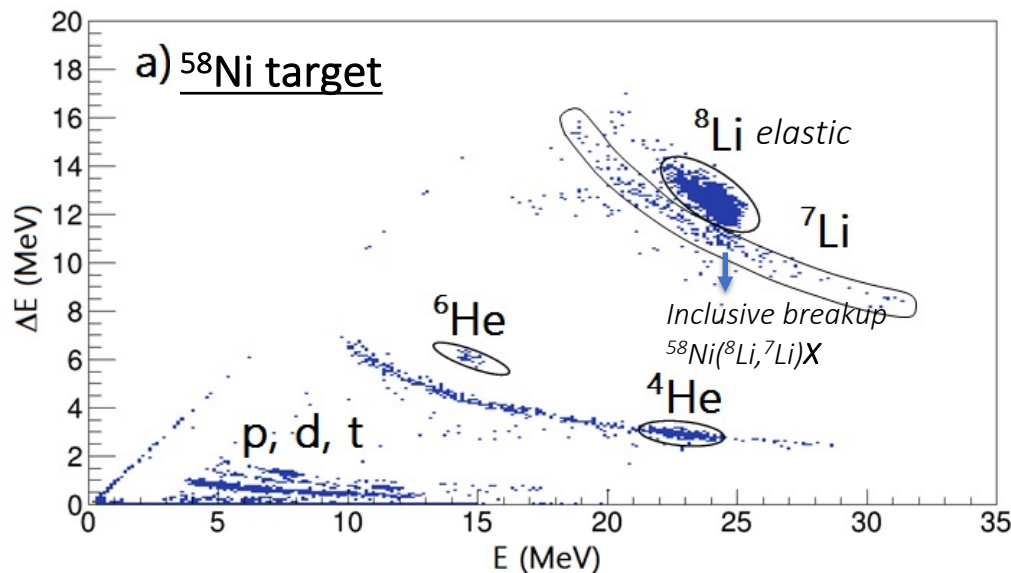
$\Delta\Omega = 30 \text{ msr}$



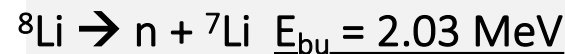
1- primary target  
 2- collimator  
 3- Faraday cup  
 4- solenoid

5- lollipop  
 6- collimator  
 7- scattering chamber, secondary target  
 and detectors

# Inclusive breakup reactions with $^8\text{Li}$ Beam: two E- $\Delta E$ identification spectra of the $^8\text{Li}+^{58}\text{Ni}$ collision

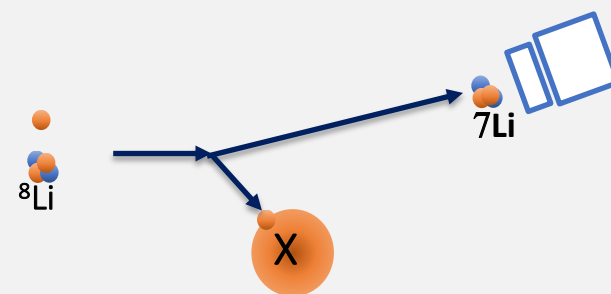


$^8\text{Li}$  is a weakly bound nucleus that breaks into a  $^7\text{Li}$  and a neutron



## Inclusive breakup reactions:

What kind of information one can get if only one of the projectiles fragment is detected

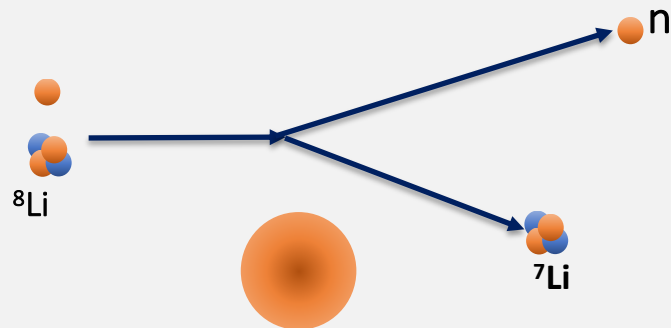


$^7\text{Li}$  energy and angular distributions

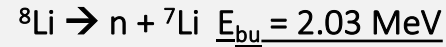


## Two different processes are possible to produce ${}^7\text{Li}$ from the ${}^8\text{Li}+{}^{58}\text{Ni}$ collision:

elastic breakup



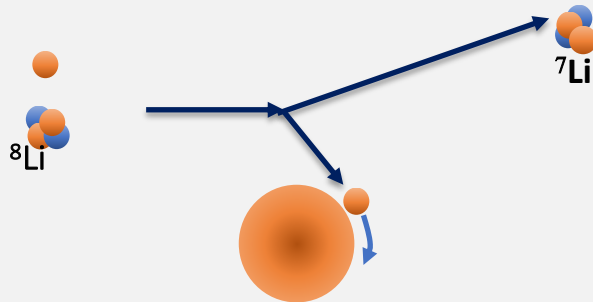
Elastic breakup:



Q-value is negative for elastic breakup

*There is a threshold at  $E_{bu}$*

neutron transfer or non-elastic breakup (NEB)



Neutron transfer or non-elastic breakup (NEB)

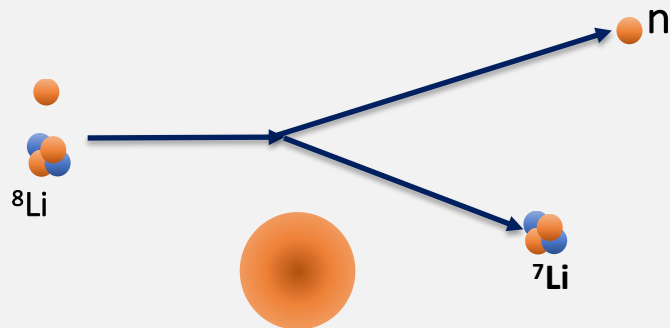
Q-value can be either positive or negative

*The transferred neutron interacts strongly with the target*

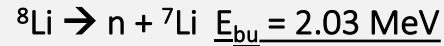
Reaction Q-value can be either positive or negative depending on the final state excitation energy

## Two different processes are possible to produce ${}^7\text{Li}$ from the ${}^8\text{Li}+{}^{58}\text{Ni}$ collision:

elastic breakup



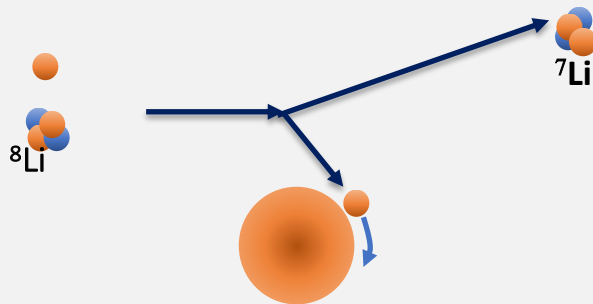
Elastic breakup:



Q-value is negative for elastic breakup

*There is a threshold at  $E_{bu}$*

neutron transfer or non-elastic breakup (NEB)

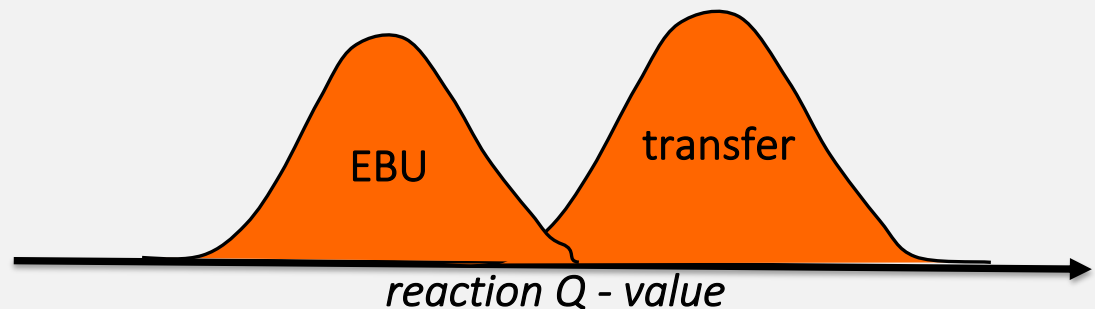


Neutron transfer or non-elastic breakup (NEB)

Q-value can be either positive or negative

*The transferred neutron interacts strongly with the target*

Reaction Q-value can be either positive or negative depending on the final state excitation energy



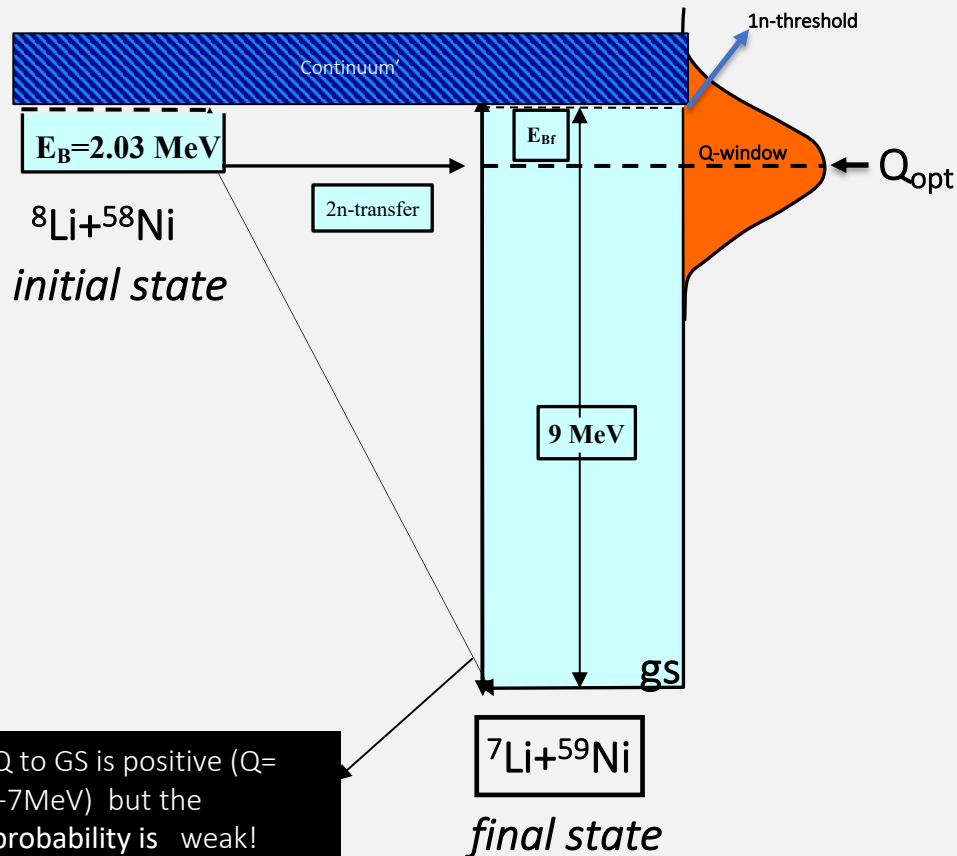
# Dynamics of the neutron transfer reactions

Transfer reactions are very selective of the final states energies and angular momentum.

Q-optimum considerations

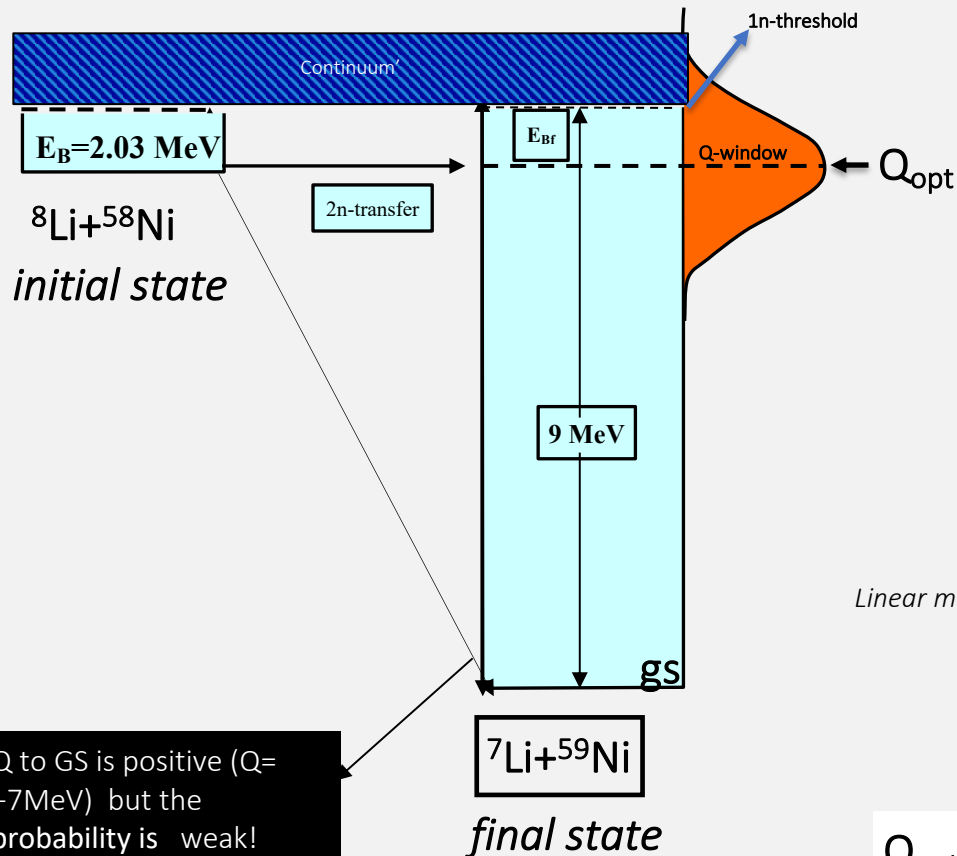
linear and angular momentum matching conditions

Seminal paper by D. M. Brink, PLB v.40, pg 37 (1972)



# Dynamics of the neutron transfer reactions

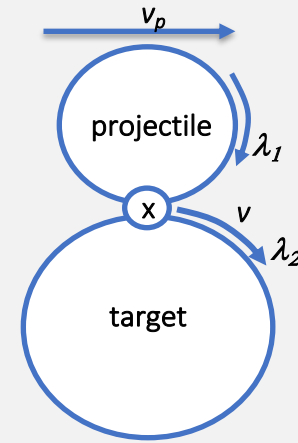
Transfer reactions are very selective of the final states energies and angular momentum.



## Q-optimum considerations

linear and angular momentum matching conditions

Seminal paper by D. M. Brink, PLB v.40, pg 37 (1972)



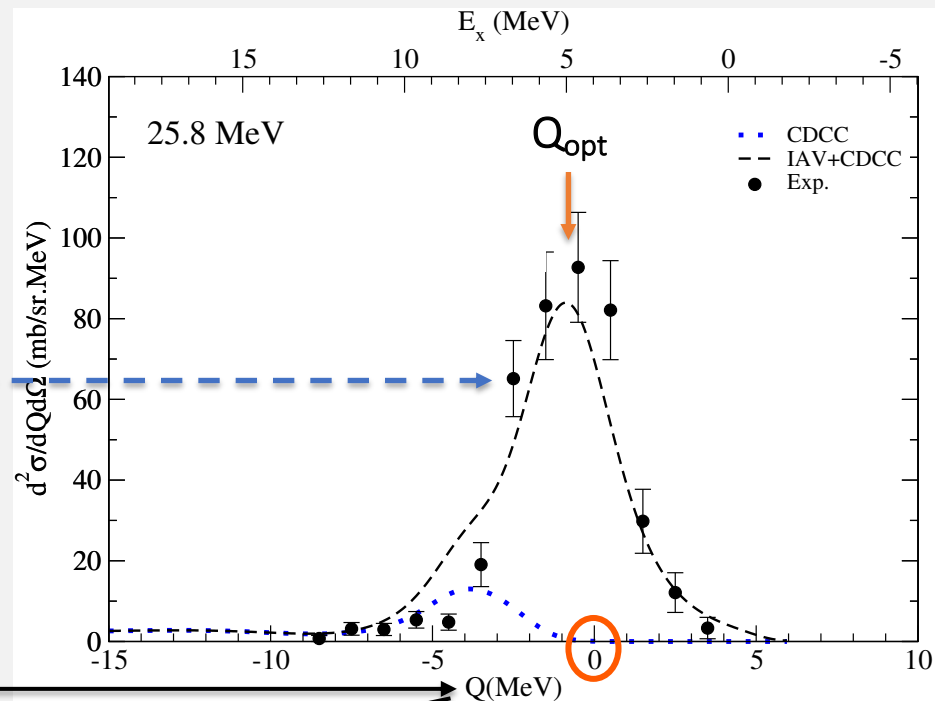
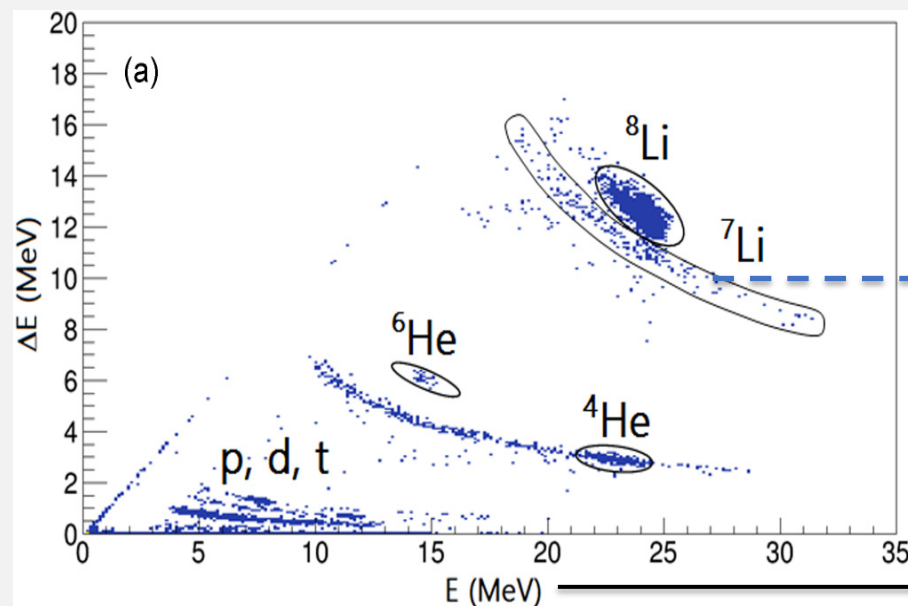
## Classical selection rules

Linear momentum of the transfer particle stays constant during the transfer

for neutron transfers  $Q_{\text{opt}} \sim 0$

$Q_{\text{opt}}$  shifts to negative values as more and more angular momentum is transferred in the collision

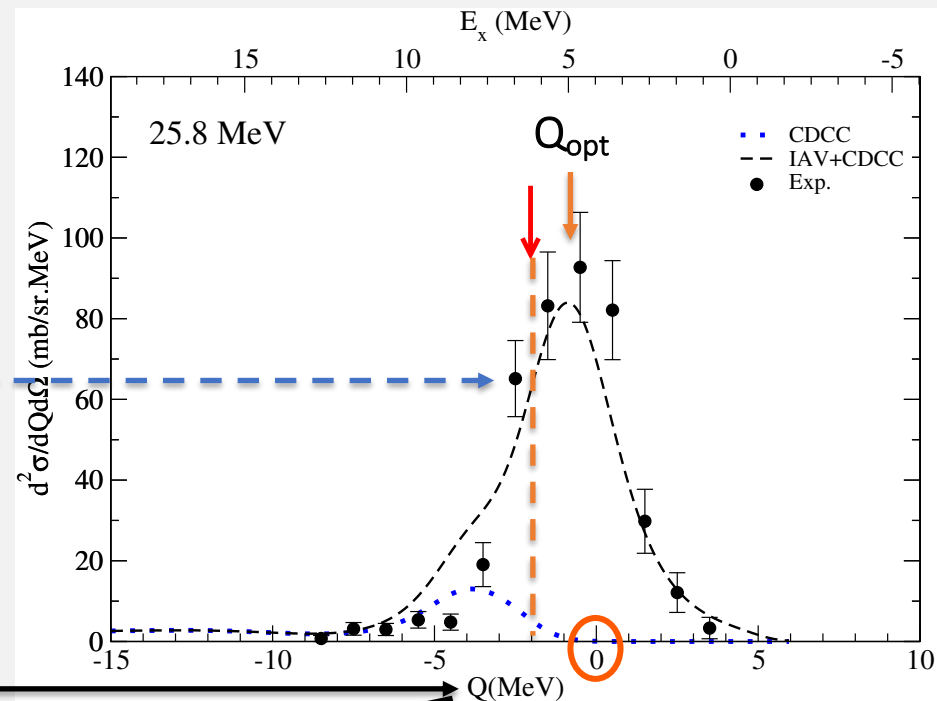
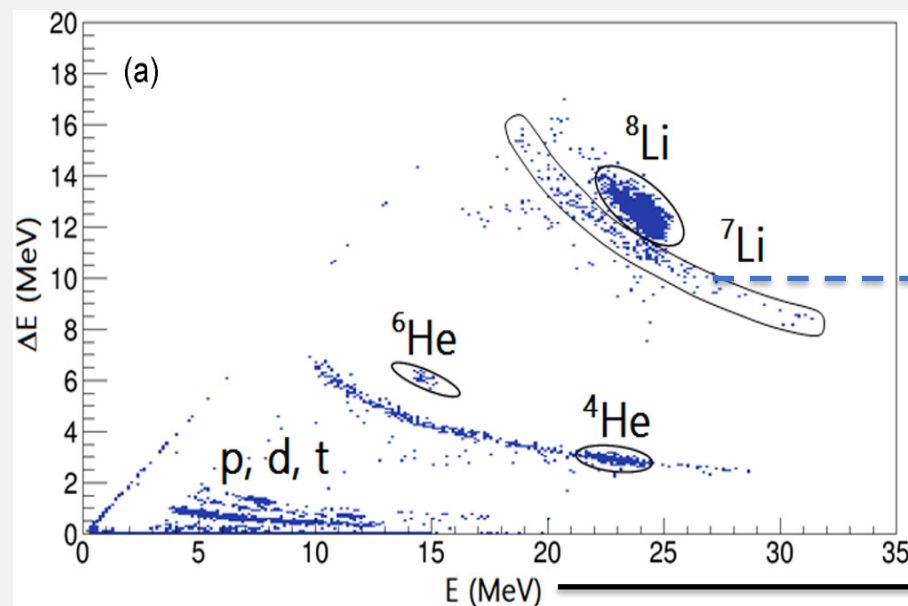
# $^7\text{Li}$ energy distribution: $A(^8\text{Li}, ^7\text{Li})X$



Transformation  $E_{^7\text{Li}} \rightarrow$  reaction  $Q$ -value

using the kinematics of the  $^{58}\text{Ni}(^8\text{Li}, ^7\text{Li})^{59}\text{Ni}^*$  reaction

# $^7\text{Li}$ energy distribution: $A(^8\text{Li}, ^7\text{Li})X$



Transformation  $E_{^7\text{Li}} \rightarrow$  reaction  $Q$ -value

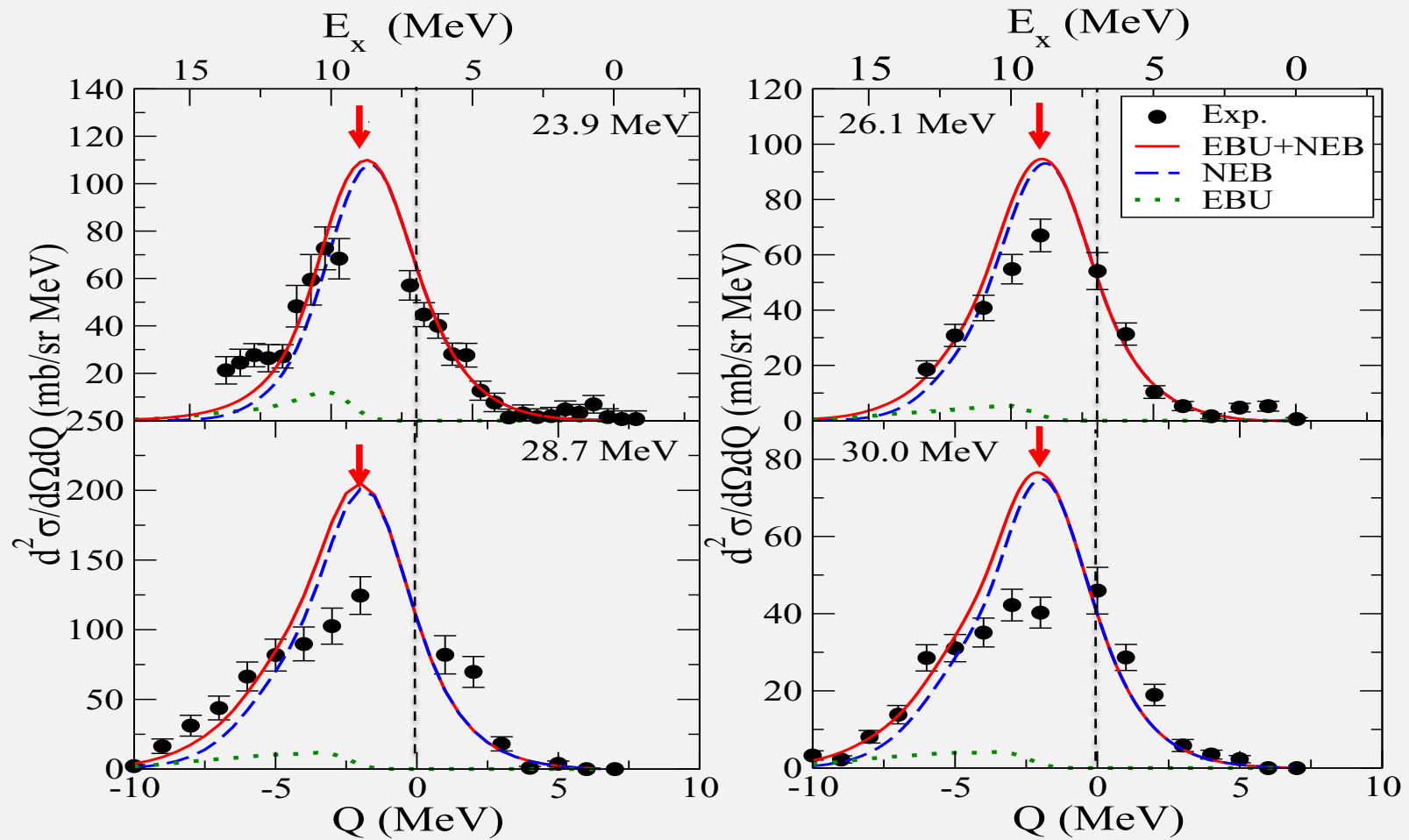
using the kinematics of the  $^{58}\text{Ni}(^8\text{Li}, ^7\text{Li})^{59}\text{Ni}^*$  reaction

Why?

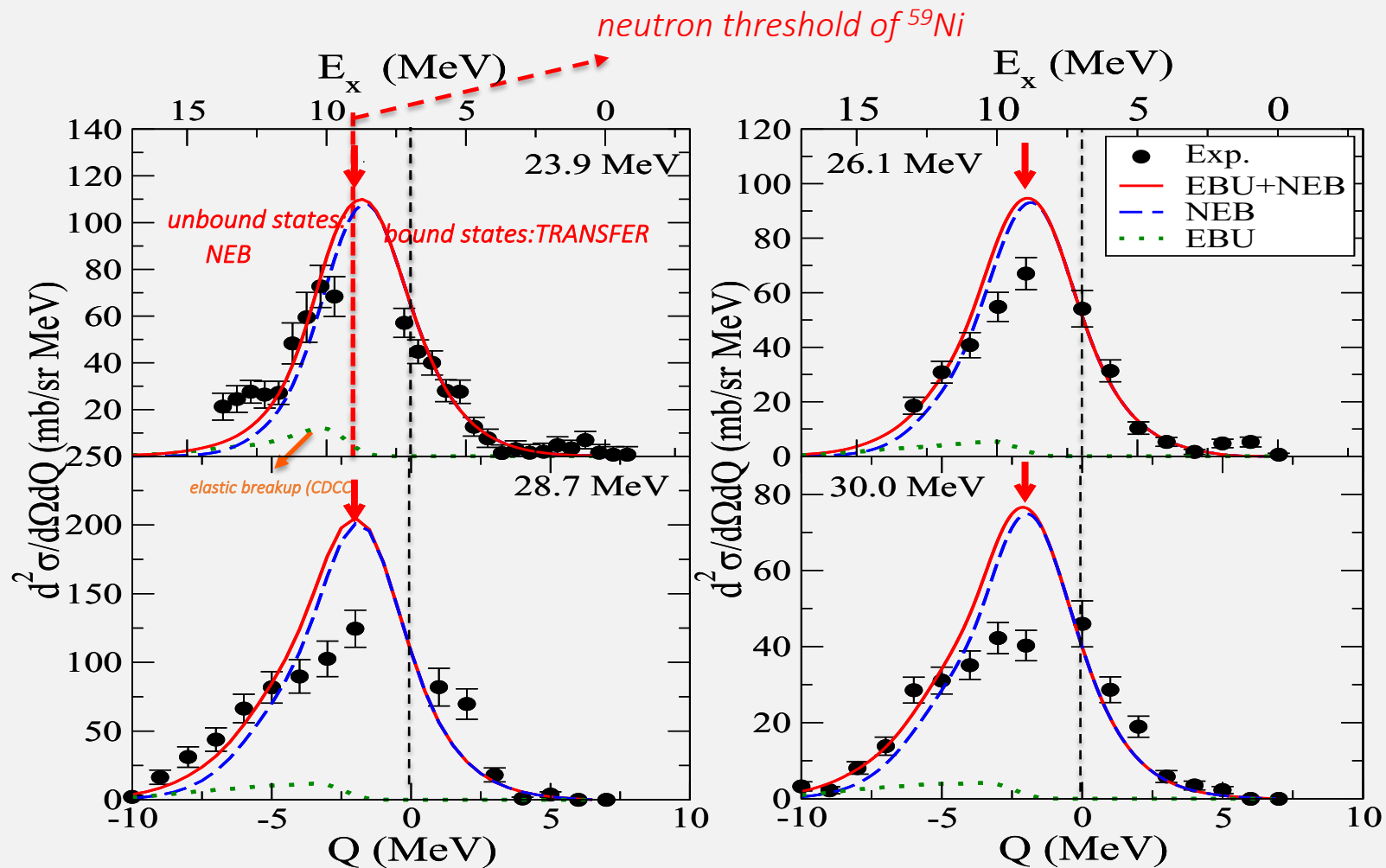
because the  $E_{^7\text{Li}}$  distribution depends on the scattering angle but  $Q$  does not.

*missing mass spectrum*

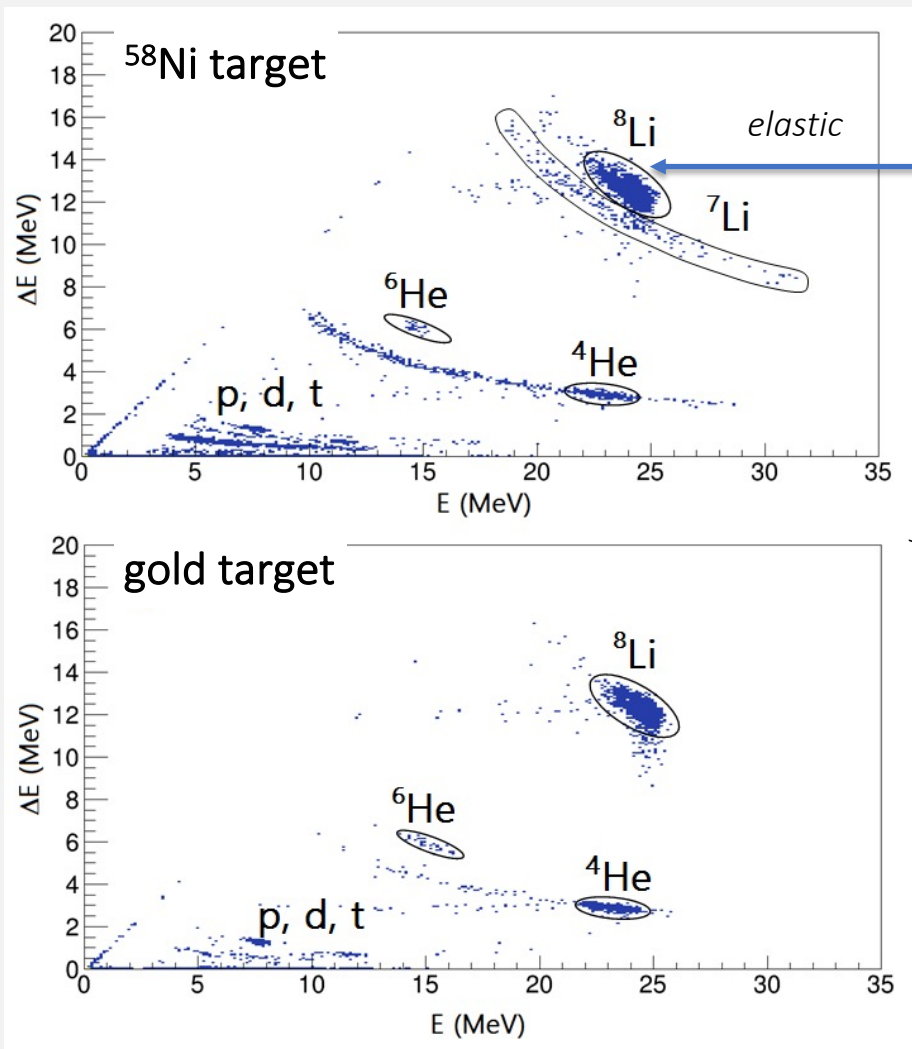




About one-half of the flux goes to bound states (transfer) and one-half to unbound states (breakup)



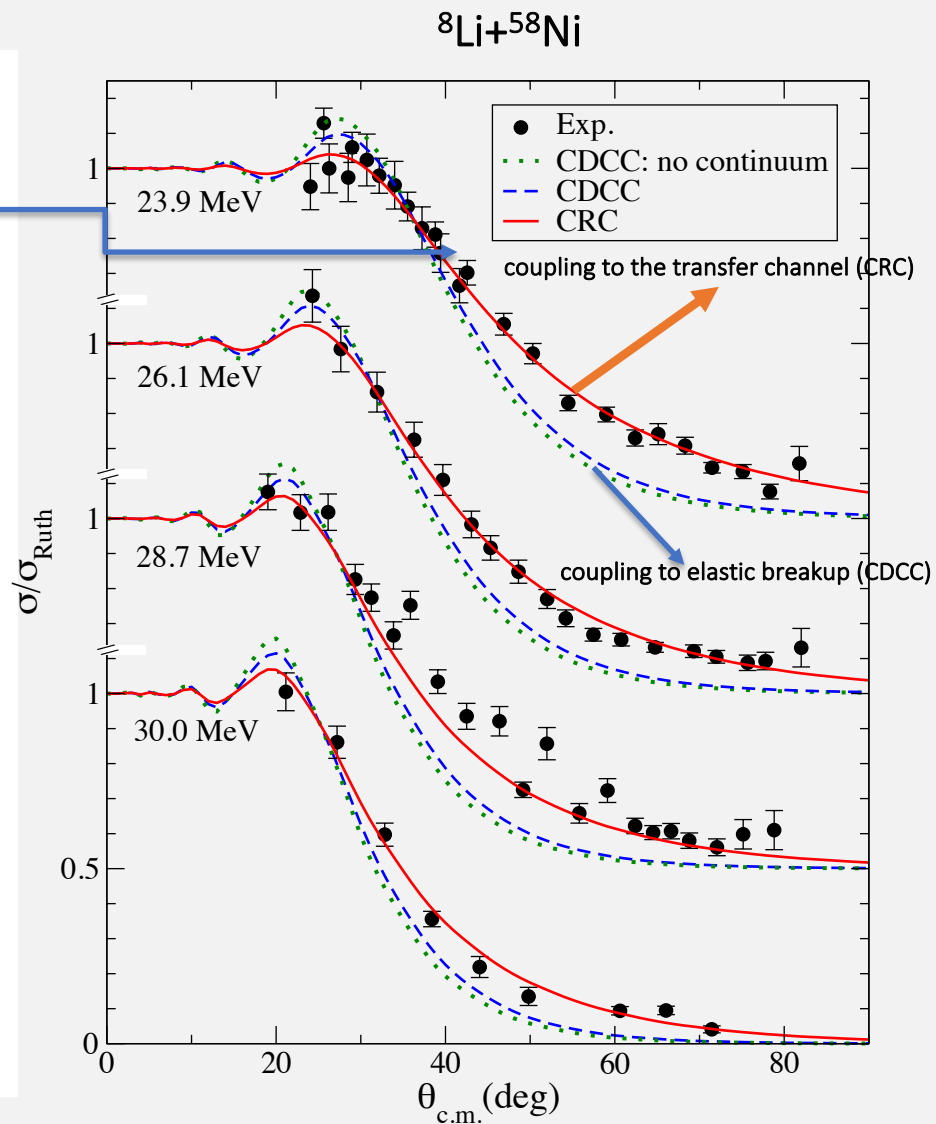
About one-half of the flux goes to bound states (transfer) and one-half to unbound states (breakup)



Physical Review C103,064601(2021)

### Evidence of Strong stripping channels in the dynamics of the $^8\text{Li}+^{58}\text{Ni}$ reaction

O.C.B. SANTOS et al.



## Calculations:

- Optical model for elastic scattering
- Continuum Discretized Coupled Channels (CDCC) for elastic scattering and elastic breakup
- Coupled Reaction Channels (CRC) for elastic scattering and transfer reactions
- Ichimura, Austern, Vincent (IAV) for transfer + breakup (NEB)

PHYSICAL REVIEW C

VOLUME 32, NUMBER 2

AUGUST 1985

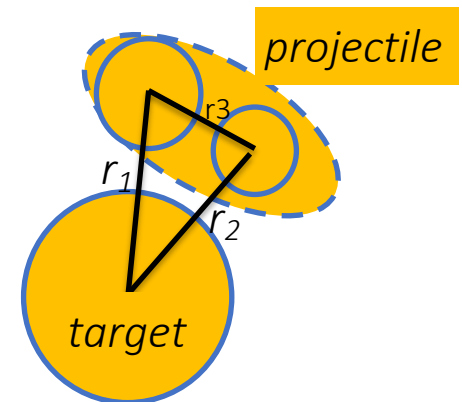
### Equivalence of post and prior sum rules for inclusive breakup reactions

M. Ichimura

*Institute of Physics, University of Tokyo, College of General Education, Komaba 3-8-1, Tokyo 153, Japan*

N. Austern and C. M. Vincent

*Department of Physics and Astronomy, University of Pittsburgh, Pittsburgh, Pennsylvania 15260*



Ingredients: fragment-target optical potentials ( $V_1$ ,  $V_2$ )

for CRC → representative excited states and spectroscopic factors

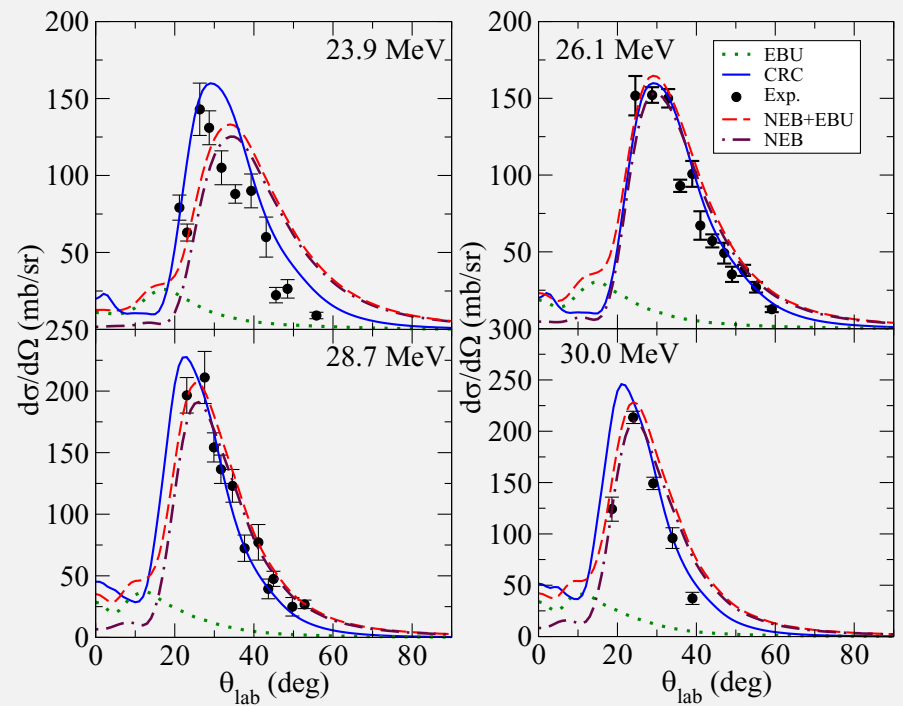
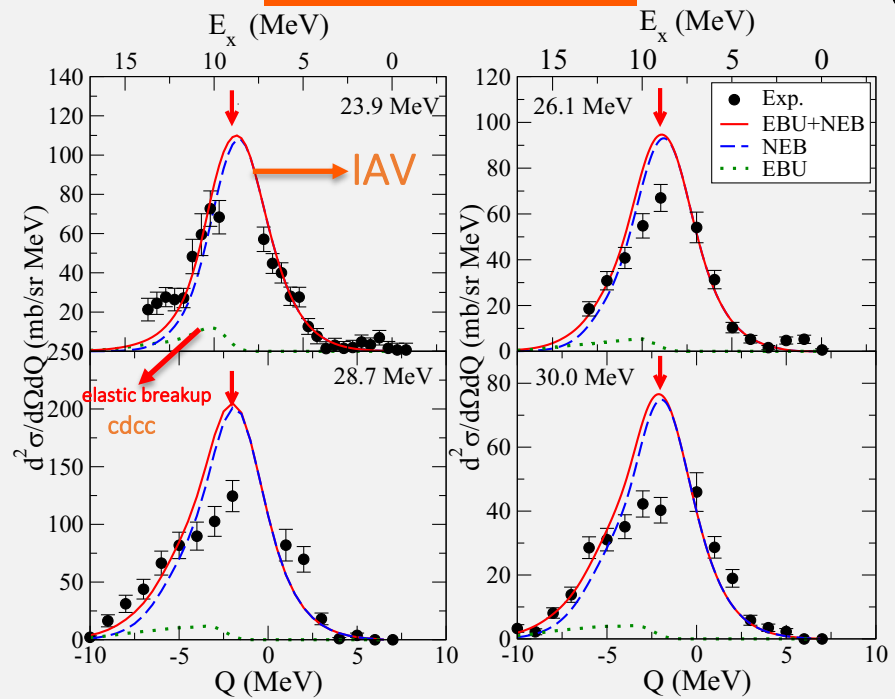
for IAV → the imaginary part of the optical potential between the transferred particle and the target.

# Energy and angular $^7\text{Li}$ distributions in the $^8\text{Li}+^{58}\text{Ni}$ reaction compared with Ichimura, Austern, Vincent (IAV) calculations.

## $^7\text{Li}$ Energy distributions

## $^{58}\text{Ni}(^8\text{Li}, ^7\text{Li})\text{X}$

## $^7\text{Li}$ Angular distributions



## No free parameters !

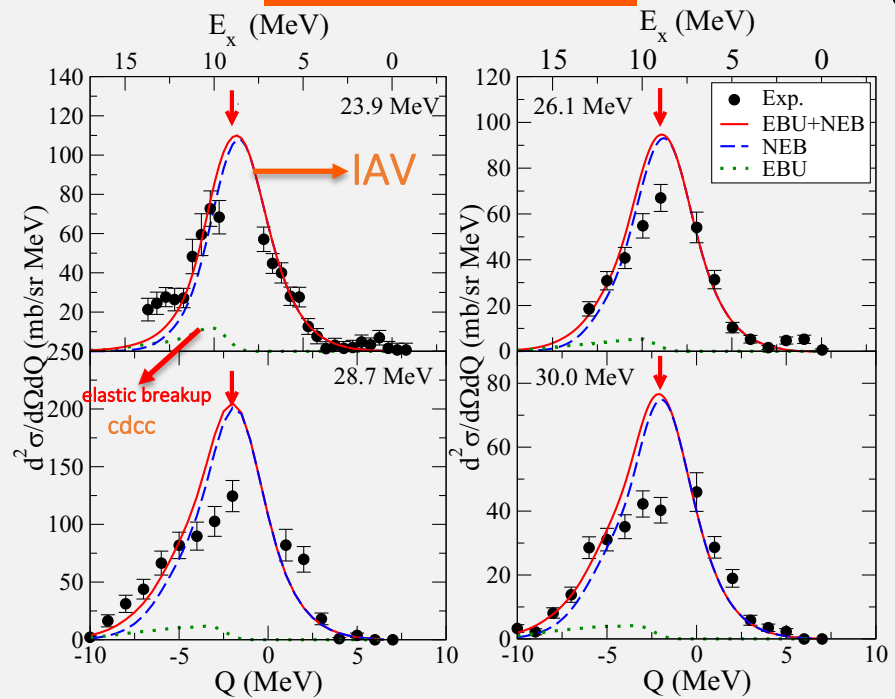
Total BU cross sections →

Energy (MeV)	$\sigma_{\text{reac}}^{\text{CRC}}$ (mb)	$\sigma_{\text{reac}}^{\text{OM-fit}}$ (mb)	$\sigma_{\text{bu}}^{\text{CRC}}$ (mb)	$\sigma_{\text{bu}}^{\text{NEB+EBU}}$ (mb)	$\sigma_{\text{bu}}^{\text{NEB}}$ (mb)
23.9	1354	1194	244	291	262
26.1	1484	1322	242	290	261
28.7	1606	1446	236	284	255
30.0	1657	1500	233	281	252

Physical Review C103,064601(2021)  
Evidence of Strong stripping channels in the dynamics of the  $^8\text{Li}+^{58}\text{Ni}$  reaction  
O.C.B. SANTOS et al.

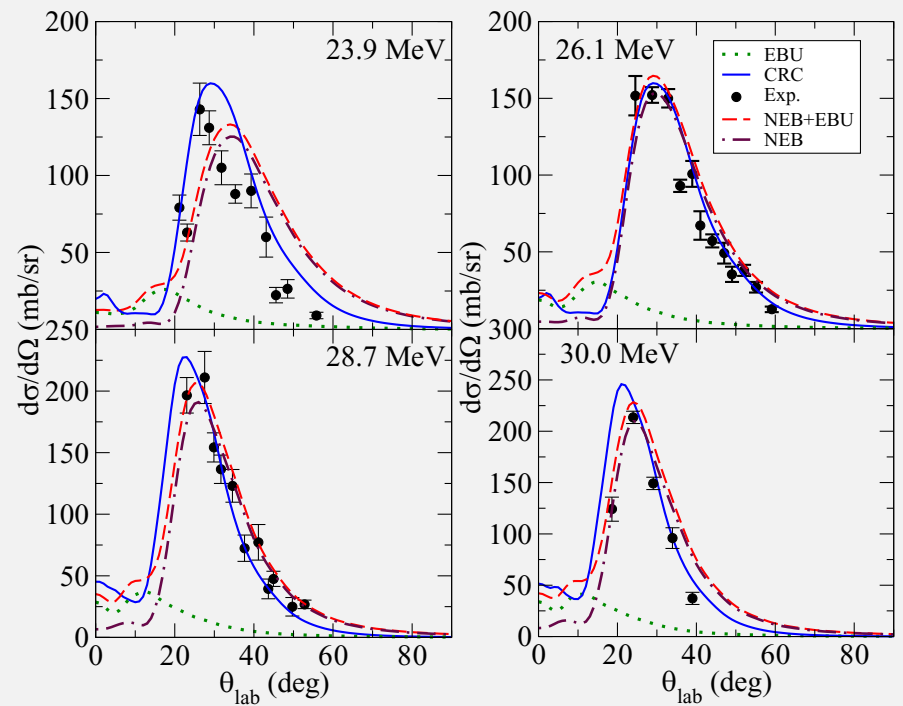
# Energy and angular $^7\text{Li}$ distributions in the $^8\text{Li}+^{58}\text{Ni}$ reaction compared with Ichimura, Austern, Vincent (IAV) calculations.

## $^7\text{Li}$ Energy distributions



## $^{58}\text{Ni}(^8\text{Li}, ^7\text{Li})\text{X}$

## $^7\text{Li}$ Angular distributions



## No free parameters !

Total BU cross sections →

Energy (MeV)	$\sigma_{\text{reac}}^{\text{CRC}}$ (mb)	$\sigma_{\text{reac}}^{\text{OM-fit}}$ (mb)	$\sigma_{\text{bu}}^{\text{CRC}}$ (mb)	$\sigma_{\text{bu}}^{\text{NEB+EBU}}$ (mb)	$\sigma_{\text{bu}}^{\text{NEB}}$ (mb)
23.9	1354	1194	244	291	262
26.1	1484	1322	242	290	261
28.7	1606	1446	236	284	255
30.0	1657	1500	233	281	252

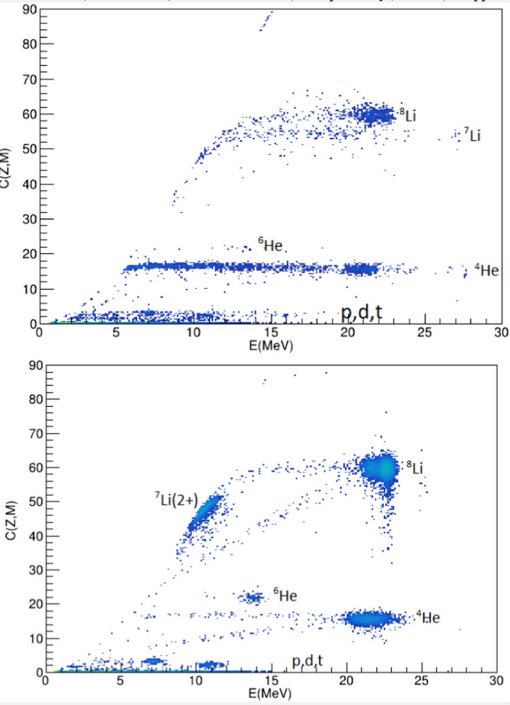
Physical Review C103,064601(2021)  
Evidence of Strong stripping channels in the dynamics of the  $^8\text{Li}+^{58}\text{Ni}$  reaction  
O.C.B. SANTOS et al.



# Light target $^8\text{Li} + ^9\text{Be}$ : $^9\text{Be}(^8\text{Li}, ^7\text{Li})^{10}\text{Be}$

## One-neutron stripping from $^8\text{Li}$ projectiles to $^9\text{Be}$ target nuclei

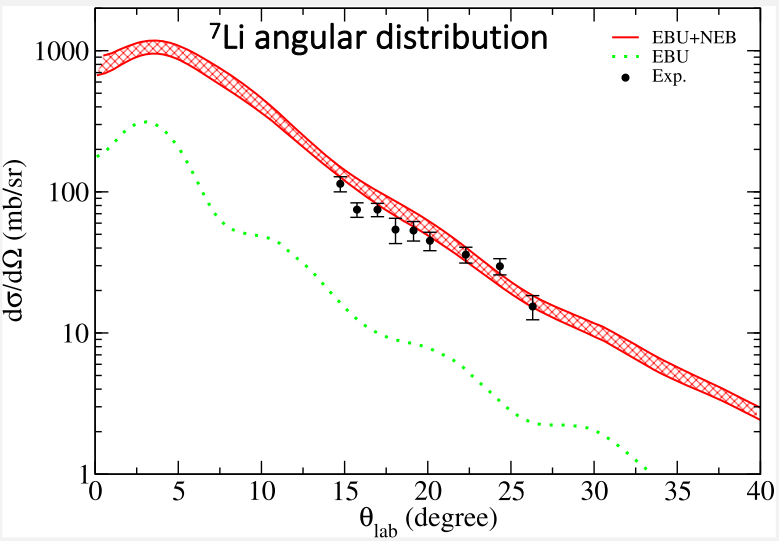
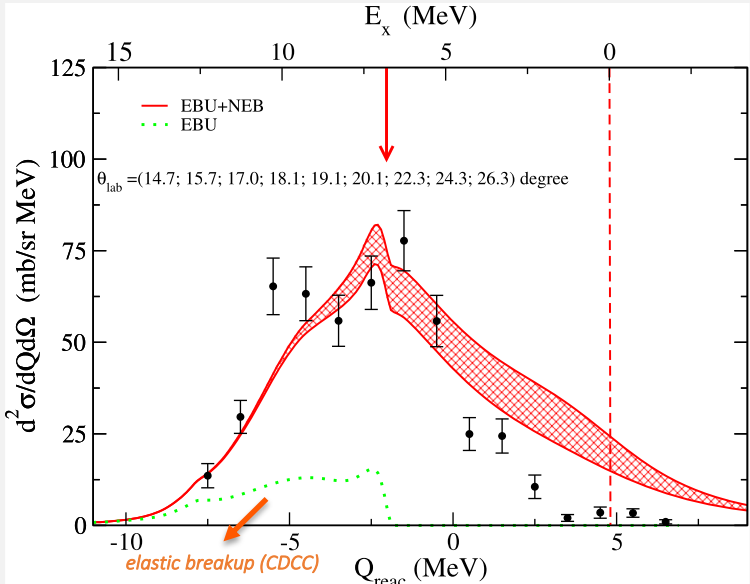
O. C. B. Santos<sup>1,a</sup>, R. Lichtenthaler<sup>1,b</sup>, A. M. Moro<sup>2,3</sup>, K. C. C. Pires<sup>1</sup>, U. Umbelino<sup>1</sup>, A. S. Serra<sup>1</sup>, E. O. N. Zevall<sup>1</sup>, A. L. de Lara<sup>1</sup>, V. Scarduelli<sup>1</sup>, J. Alcantara-Nuez<sup>1</sup>, A. Lepine-Szily<sup>1</sup>, Jin Lei<sup>4</sup>, S. Appannababu<sup>5</sup>, M. Assuno<sup>6</sup>



TRCS=1440 mb  
Total-Bu-cs=130 mb

Elastic breakup gives small contribution

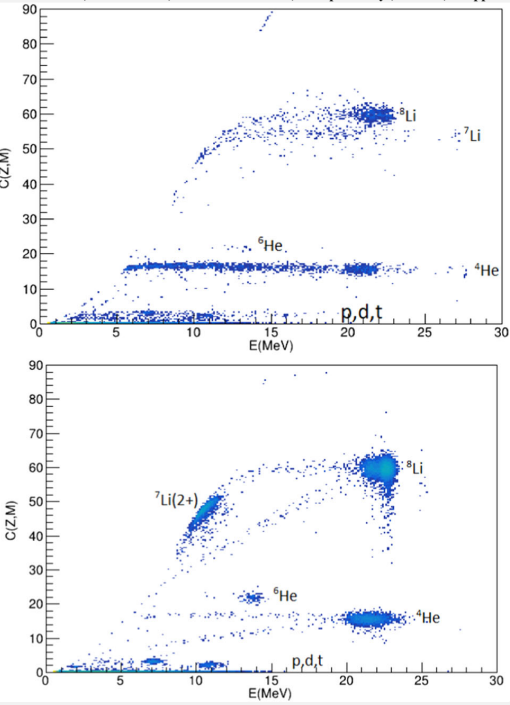
## $^7\text{Li}$ energy distribution



# Light target $^8\text{Li} + ^9\text{Be}$ : $^9\text{Be}(^8\text{Li}, ^7\text{Li})^{10}\text{Be}$

## One-neutron stripping from $^8\text{Li}$ projectiles to $^9\text{Be}$ target nuclei

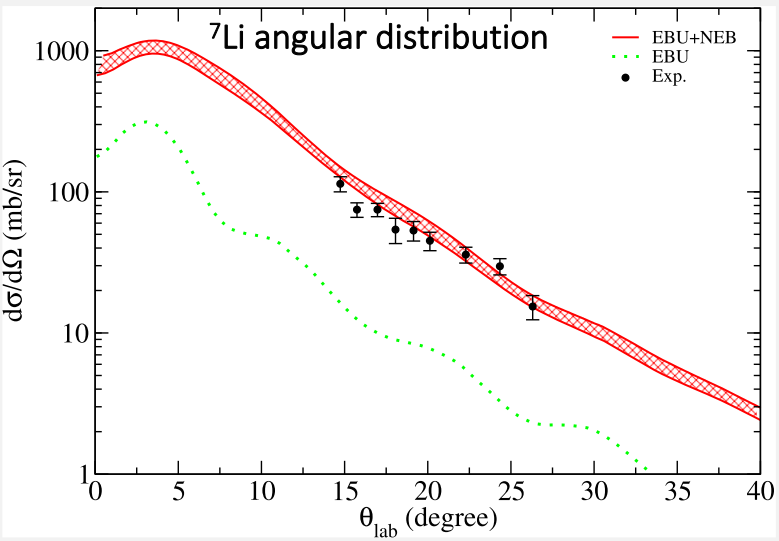
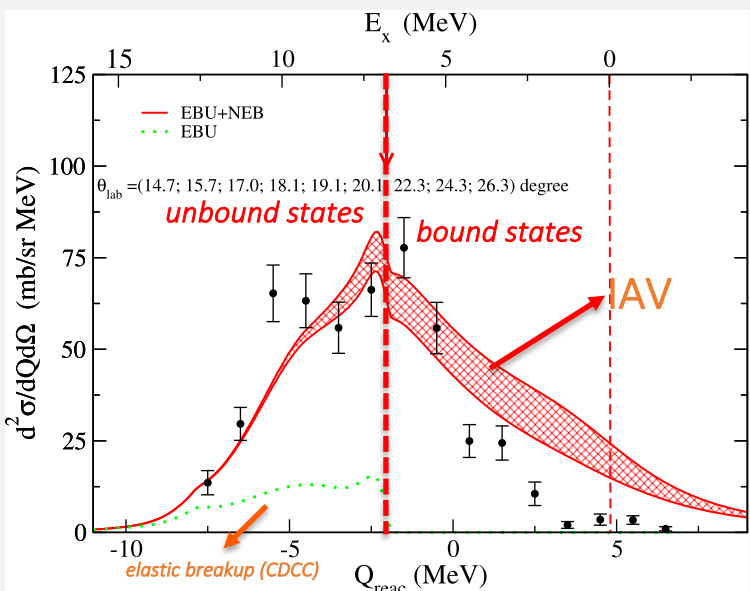
O. C. B. Santos<sup>1,a</sup>, R. Lichtenthaler<sup>1,b</sup>, A. M. Moro<sup>2,3</sup>, K. C. C. Pires<sup>1</sup>, U. Umbelino<sup>1</sup>, A. S. Serra<sup>1</sup>, E. O. N. Zevallo<sup>1</sup>, A. L. de Lara<sup>1</sup>, V. Scarduelli<sup>1</sup>, J. Alcantara-Nunez<sup>1</sup>, A. Lepine-Szily<sup>1</sup>, Jin Lei<sup>4</sup>, S. Appannababu<sup>5</sup>, M. Assuncao<sup>6</sup>



TRCS=1440 mb  
Total-Bu-cs=130 mb

Elastic breakup gives small contribution

## $^7\text{Li}$ energy distribution



# $^8\text{Li}$ on a heavy target: $^{120}\text{Sn}(^8\text{Li}, ^7\text{Li})^{121}\text{Sn}$

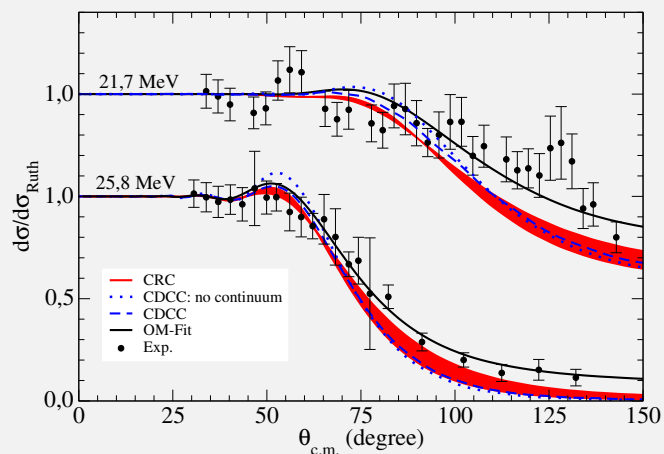
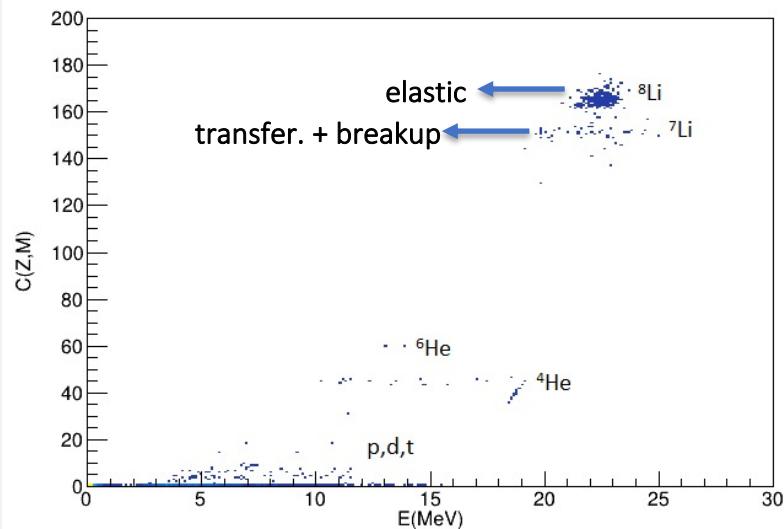
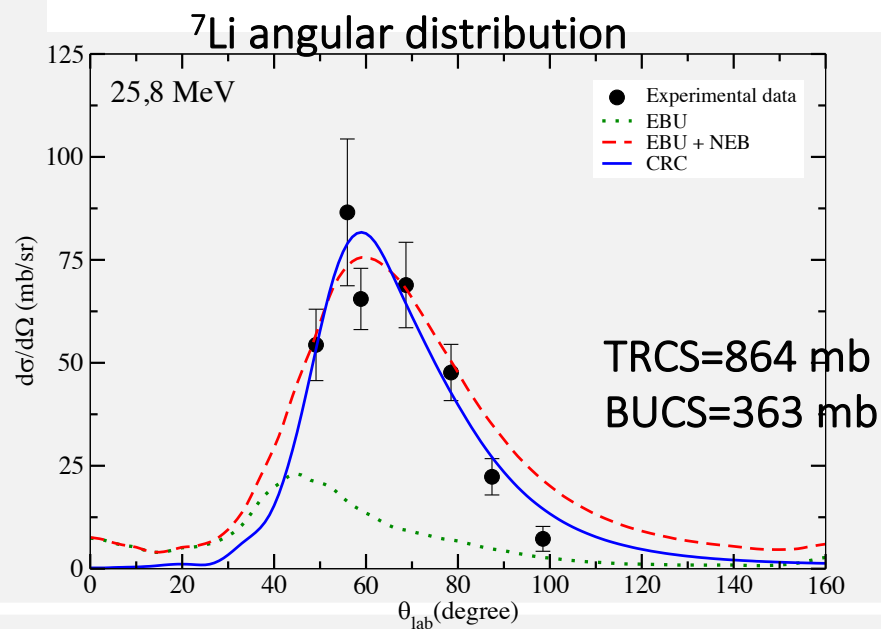
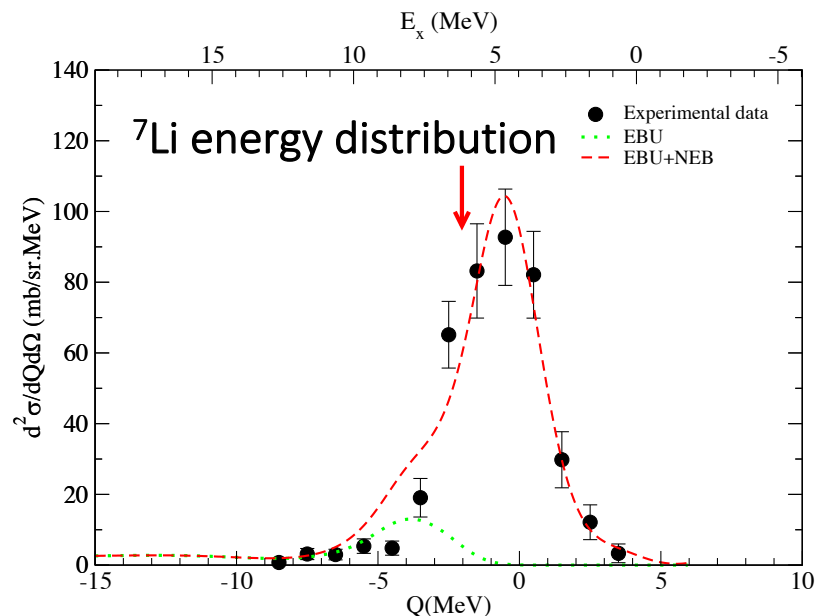


FIG. 2.  $^8\text{Li} + ^{120}\text{Sn}$  experimental elastic scattering angular distributions compared with the CDCC no-continuum (dotted blue line), full CDCC (dashed blue line), CRC (solid red line), and OM-Fit (solid black line).



# $^8\text{Li}$ on a heavy target: $^{120}\text{Sn}(^8\text{Li}, ^7\text{Li})^{121}\text{Sn}$

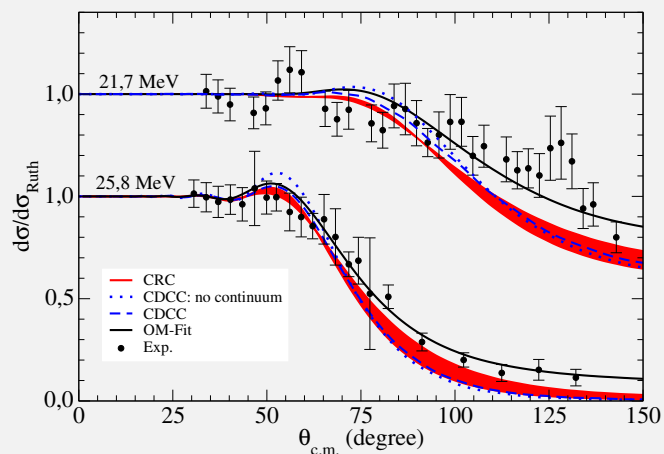
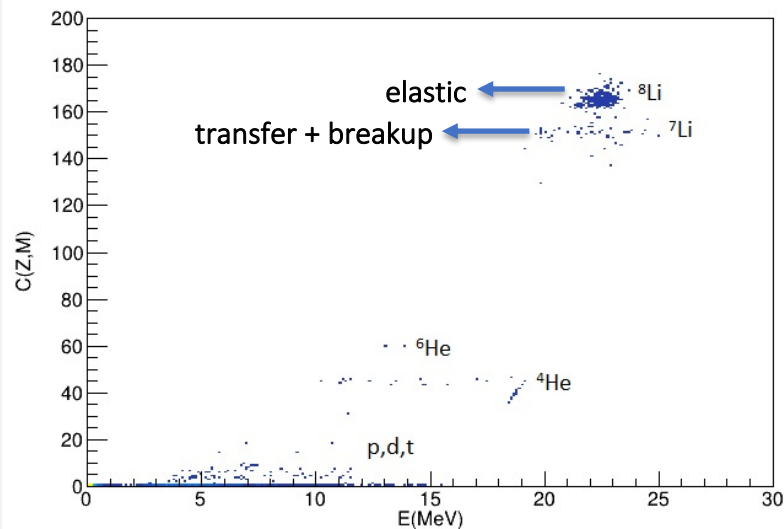


FIG. 2.  $^8\text{Li} + ^{120}\text{Sn}$  experimental elastic scattering angular distributions compared with the CDCC no-continuum (dotted blue line), full CDCC (dashed blue line), CRC (solid red line), and OM-Fit (solid black line).

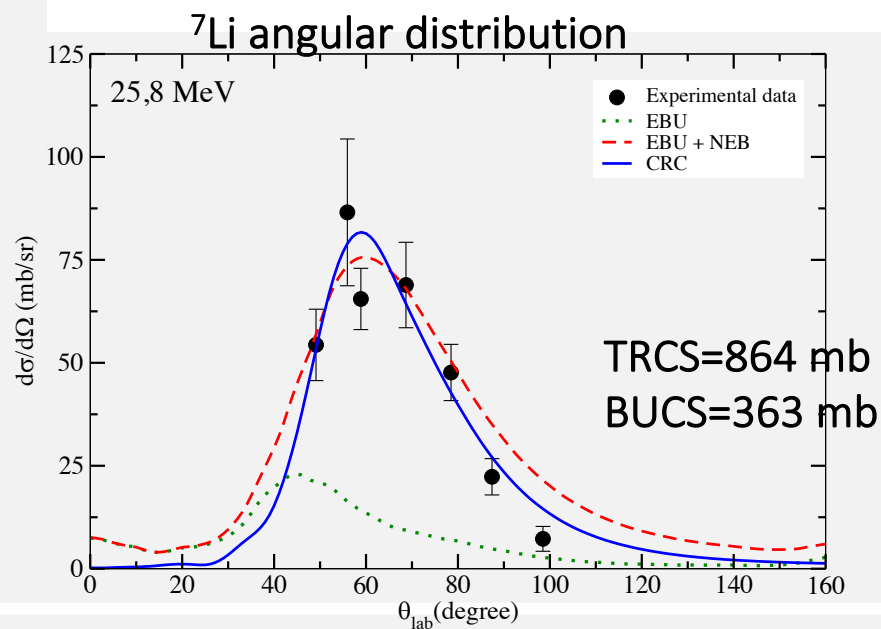
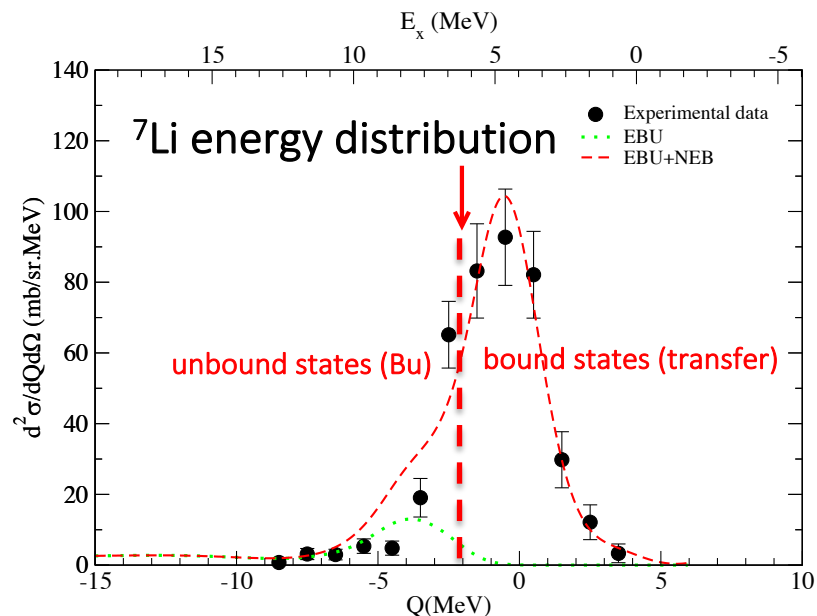
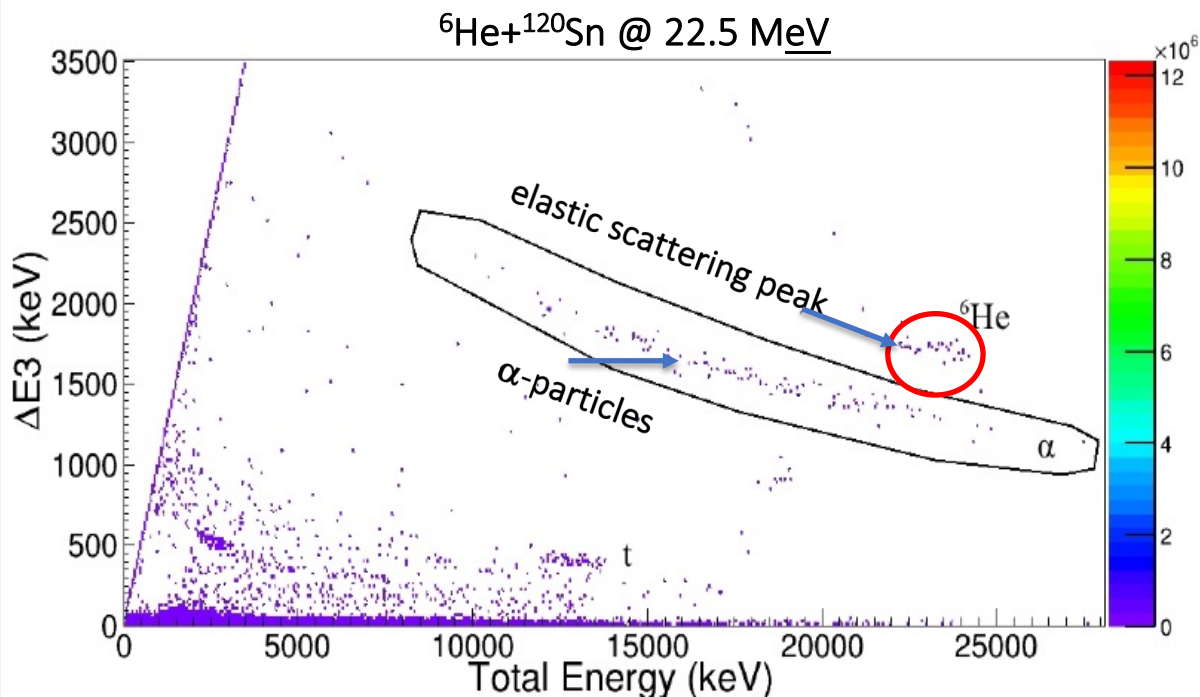


TABLE III. Total (angle integrated) breakup cross sections ( $\sigma_{\text{bu}}$ ) and total reaction cross section for  $^8\text{Li}$  on  $^9\text{Be}$  [1],  $^{58}\text{Ni}$  [2], and  $^{120}\text{Sn}$  targets.

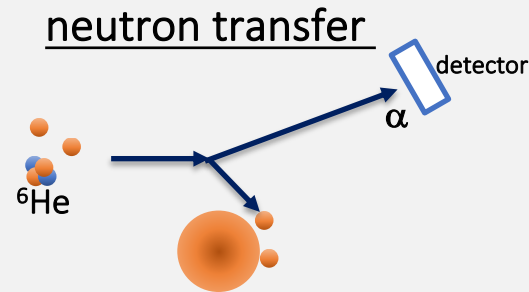
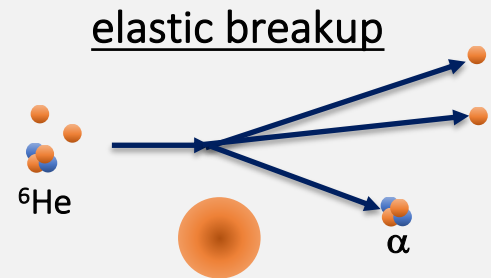
System	$E_{\text{Lab}}$ (MeV)	$\sigma_{\text{bu}}^{\text{CRC}}$ (mb)	$\sigma_{\text{bu}}^{\text{IAV+CDCC}}$ (mb)	$\sigma_{\text{reac.}}^{\text{OM}}$ (mb)	$\sigma_{\text{reac.}}^{\text{CRC}}$ (mb)	$\sigma_{\text{bu}}/\sigma_{\text{reac}}$	E/Vb
$^8\text{Li}+^9\text{Be}$	23.8	-	124(5)	1440	-	0.0861(35)	6.76
$^8\text{Li}+^{58}\text{Ni}$	23.9	244	291	1194	1354	0.210(23)	1.76
$^8\text{Li}+^{58}\text{Ni}$	26.1	242	290	1322	1484	0.190(20)	1.93
$^8\text{Li}+^{58}\text{Ni}$	28.7	236	284	1446	1606	0.170(18)	2.112
$^8\text{Li}+^{58}\text{Ni}$	30.0	233	281	1500	1657	0.163(17)	2.21
$^8\text{Li}+^{120}\text{Sn}$	21.7	267(6)	271	316	565(11)	0.842(16)	1.06
$^8\text{Li}+^{120}\text{Sn}$	25.8	291(4)	325	816	1077(25)	0.375(26)	1.26

# Alpha particle production in ${}^6\text{He}$ induced reactions

Large alpha particle yield observed in  ${}^6\text{He} + {}^{120}\text{Sn}$  collision  
- breakup or neutron transfer reactions?



Is it possible to distinguish between different processes just by detecting the alpha-particle distributions?



Possible processes:

$X = n + n + {}^{120}\text{Sn}$ ; elastic breakup

$X = n + {}^{121}\text{Sn}^*$ ; 1 neutron transfer

$X = {}^{122}\text{Sn}^*$ ; 2 neutron transfer

$X = {}^{126}\text{Te}^* \rightarrow \alpha$  complete fusion  
 $n$   
 $p$   
 $\cdot$   
 $\cdot$



# $^{120}\text{Sn}(^6\text{He},\alpha)\text{X}$ breakup or transfer?

Q-optimum considerations  
linear and angular momentum matching conditions

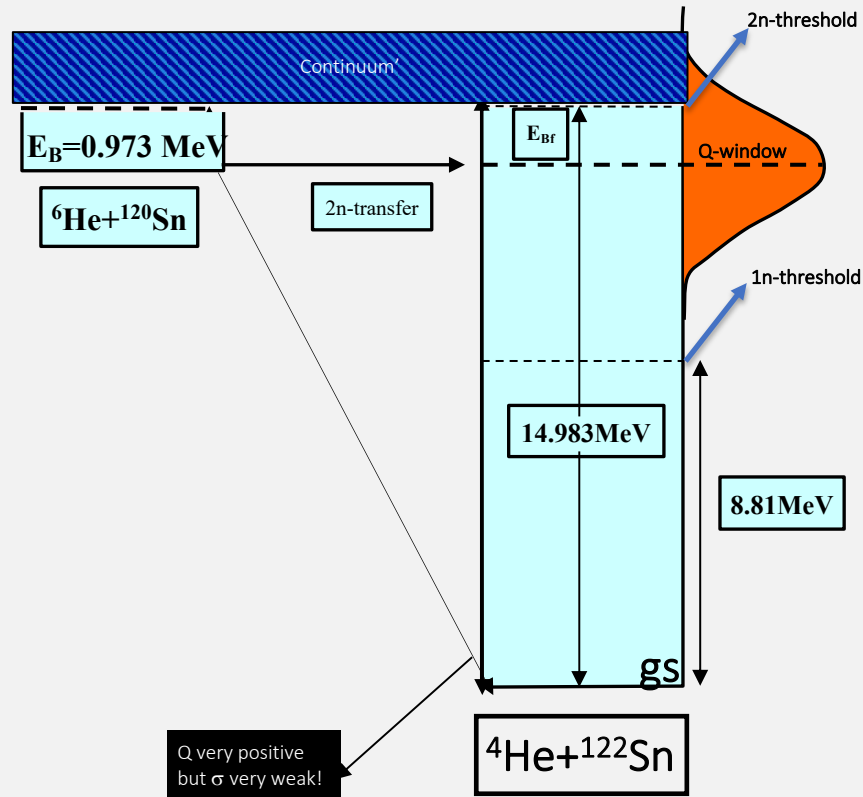
**Qopt $\approx$ 0 for neutron transfer**

*D. M. Brink, PLB v.40, pg 37 (1972)*

The transfer process is very selective in terms of the excitation energies in the final nucleus. It will favour transfer to states around the optimum- $Q_{\text{value}}$  which is determined by momentum matching conditions (Brink, 1972). In particular, for neutron transfers, the optimum Q-value is located around  $Q\approx 0$ .

## Alpha-particle energy distributions @ 60 deg

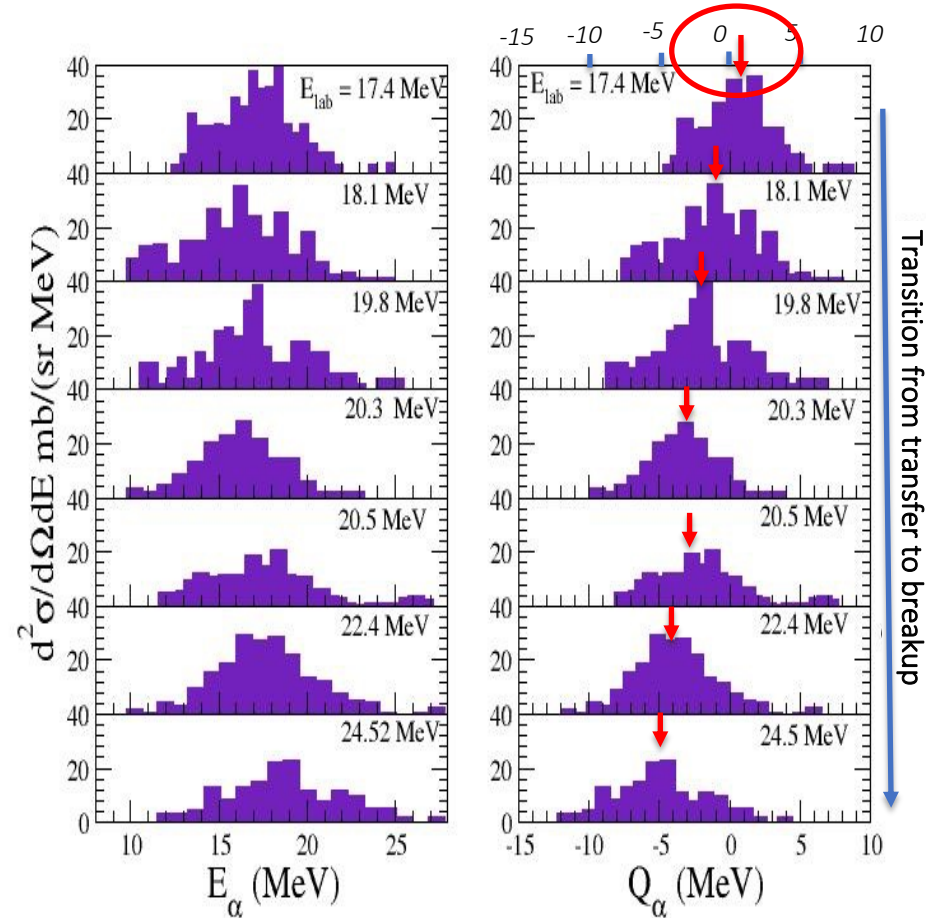
$E_\alpha \rightarrow Q$  transformation —  $^{120}\text{Sn}(^6\text{He}, \alpha)^{122}\text{Sn}^*$



Two-neutron transfer in the  $^6\text{He} + ^{120}\text{Sn}$  reaction

S. Appannababu,<sup>1,\*</sup> R. Lichtenthaler,<sup>1</sup> M. A. G. Alvarez,<sup>2</sup> M. Rodrıguez-Gallardo,<sup>2</sup> A. Lepine-Szily,<sup>1</sup> K. C. C. Pires,<sup>1</sup>

PHYSICAL REVIEW C **99**, 014601 (2019)



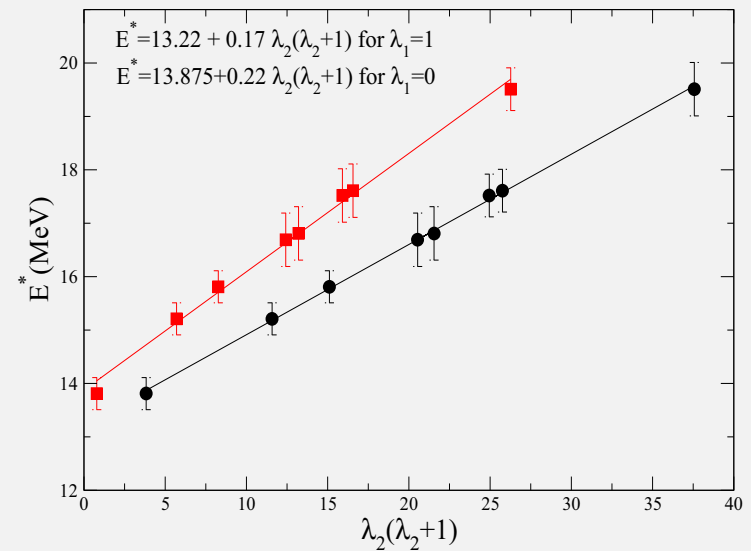
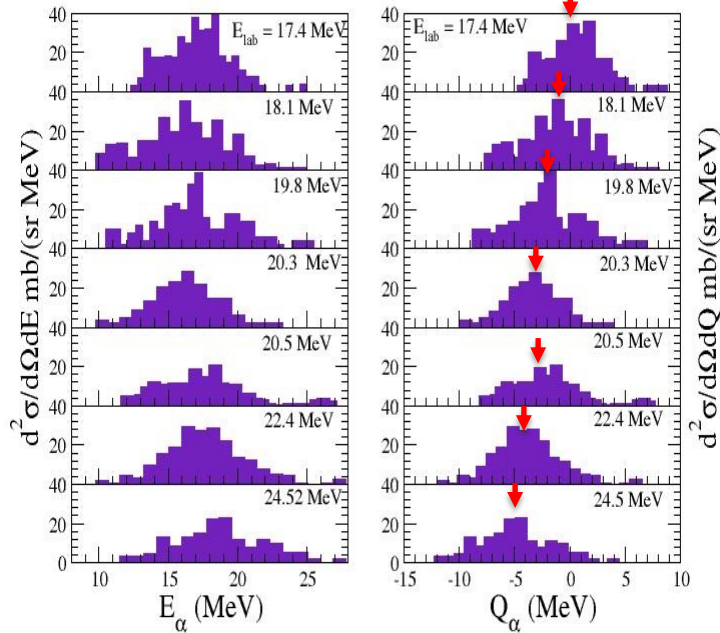
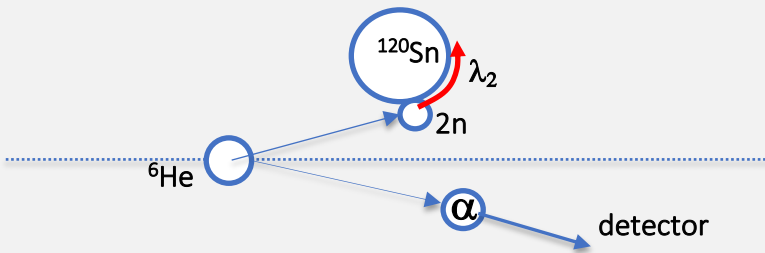
$E_\alpha \rightarrow Q$  transformation —  $^{120}\text{Sn}(^6\text{He}, \alpha)^{122}\text{Sn}^*$ 


FIG. 7. Excitation energy of the final nucleus as a function of the square of the angular momentum in the final nucleus for  $\lambda_1 = 1$  (dots) and  $\lambda_1 = 0$  (squares). The solid line is a linear fit (see text).



Two-neutron transfer in the  $^6\text{He} + ^{120}\text{Sn}$  reaction

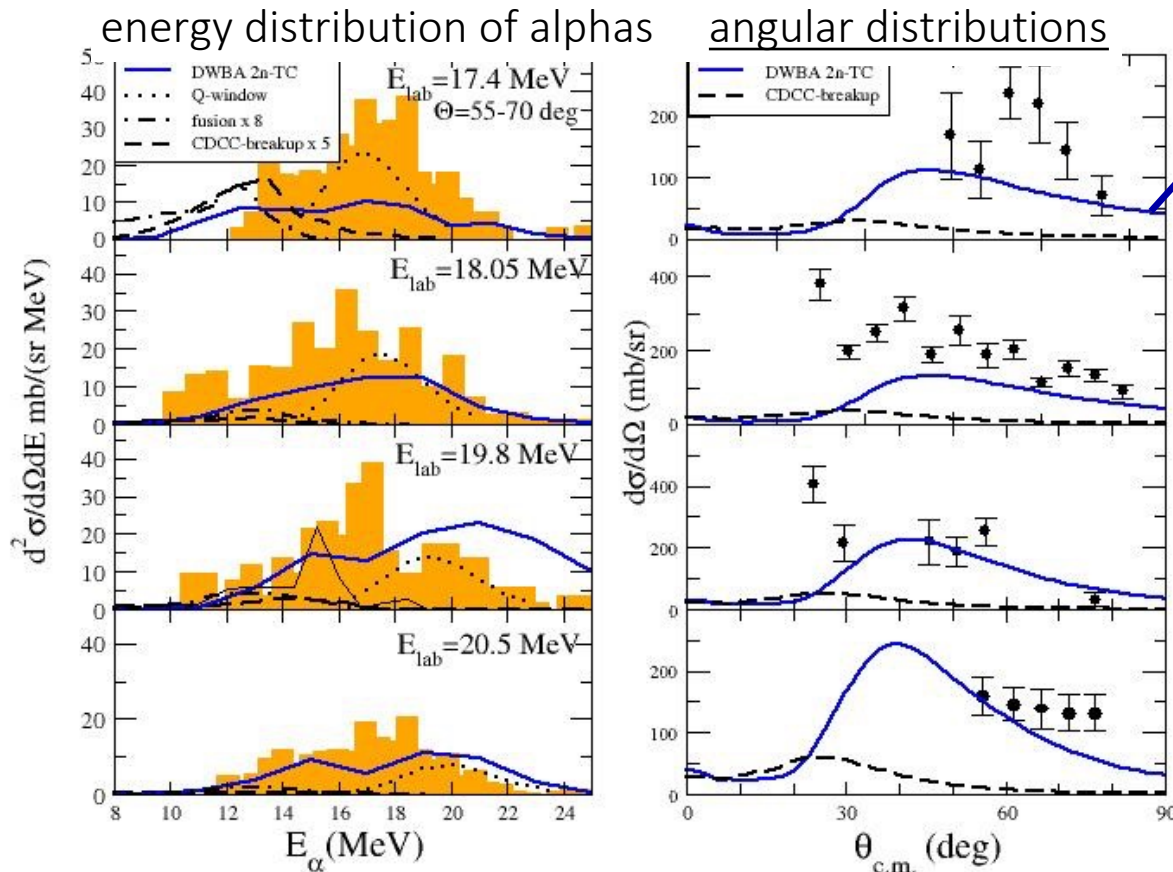
S. Appannababu,<sup>1,\*</sup> R. Lichtenthaler,<sup>1</sup> M. A. G. lvarez,<sup>2</sup> M. Rodrguez-Gallardo,<sup>2</sup> A. Lpne-Szily,<sup>1</sup> K. C. C. Pires,<sup>1</sup>

PHYSICAL REVIEW C **99**, 014601 (2019)

The present results show, for  $\lambda_1 = 1$  (dots), a linear relation between the excitation energy of the recoil nuclei and its angular momentum square  $\lambda_2(\lambda_2 + 1)$ . This seems to behave as a typical rotational band with  $K = 13.22$  MeV and a slope  $\hbar^2/(2I) = 0.17$  MeV which is very close to that expected for a rotating  $2n$ - $^{120}\text{Sn}$  system with a moment of inertia  $I = \mu R^2$  where  $\mu$  is the reduced mass of the  $^{120}\text{Sn}$ - $2n$  dinuclear system and  $R = 1.2(120^{1/3} + 2^{1/3})$  fm.

The present results indicate that the experimental  $\alpha$ -energy distributions are consistent with the formation of composite  $2n$ - $^{120}\text{Sn}$  rotating system driven by the momentum of the transferred particle ( $2n$ ).

# Alpha particles from the ${}^6\text{He}+{}^{120}\text{Sn}$ collision: DWBA for the angular distributions



- *P. N. de Faria et. al, Phys. Rev. C 82, 034602 (2010)*

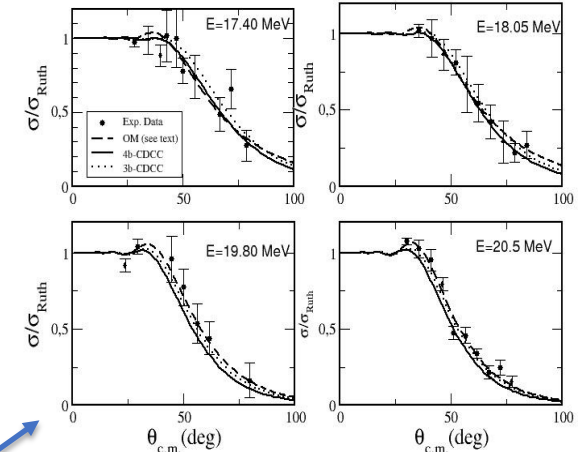
total alpha-cross section

650 mb

Total reaction cross section: 1300-1500 mb

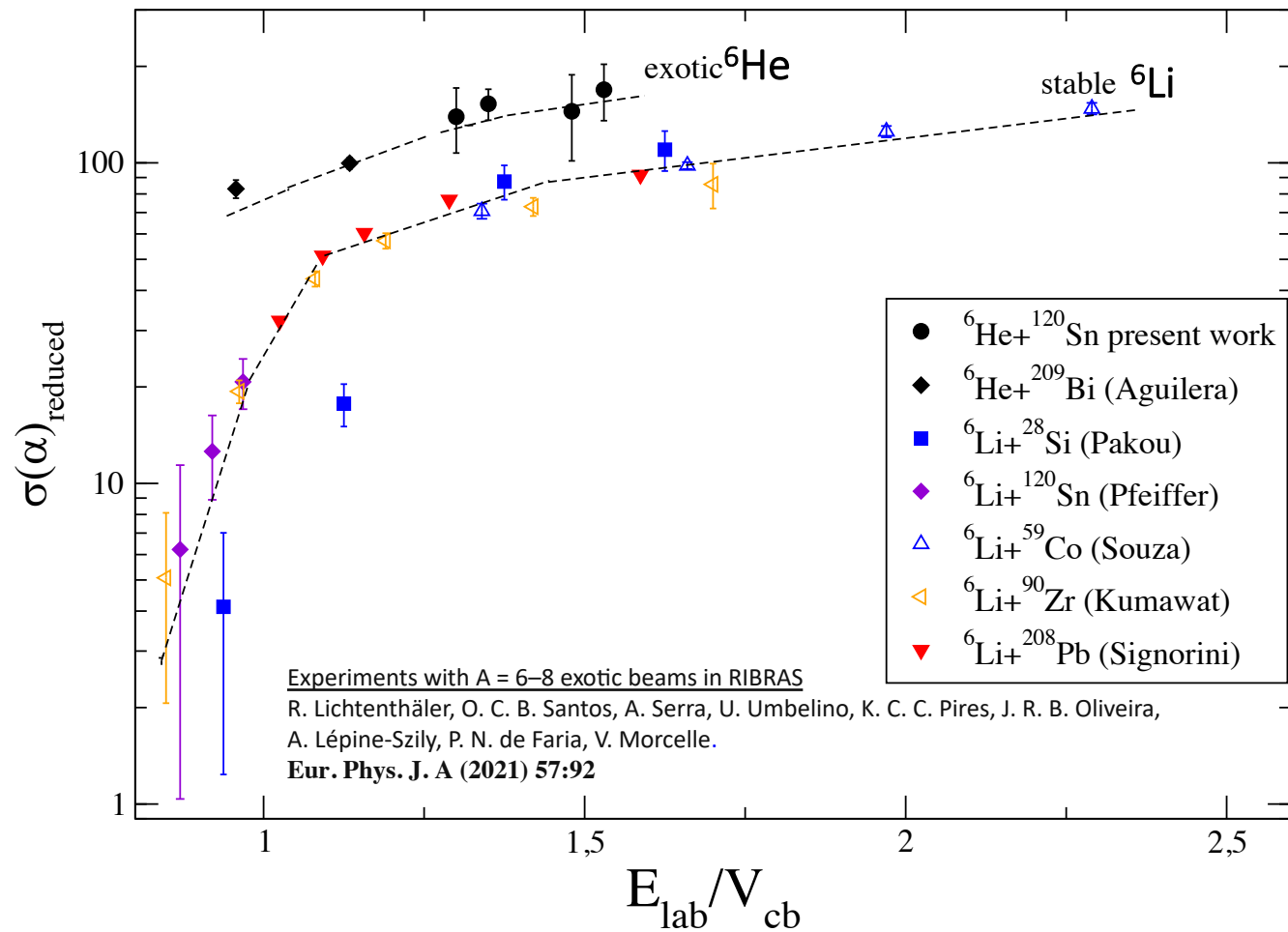
DWBA 2n-transfer to continuum and bound states (calculations by A. Moro)

## ${}^6\text{He}+{}^{120}\text{Sn}$ elastic scattering



CDCC reproduces very well the  ${}^6\text{He}+{}^{120}\text{Sn}$  angular distributions (elastic scattering) but not the large alpha particle yields observed in the  ${}^{120}\text{Sn}({}^6\text{He},\alpha)\text{X}$  reaction. CDCC description does not provide a complete description of the problem.

## Alpha particle production cross section in ${}^6\text{He}$ and ${}^6\text{Li}$ induced reactions



## $^{11}\text{Li}$ Breakup on $^{208}\text{Pb}$ at Energies Around the Coulomb Barrier

J. P. Fernández-García,<sup>1,2</sup> M. Cubero,<sup>3,4</sup> M. Rodríguez-Gallardo,<sup>1</sup> L. Acosta,<sup>5,6</sup> M. Alcorta,<sup>3</sup> M. A. G. Alvarez,<sup>1,2</sup> M. J. G. Borge,<sup>3</sup> L. Buchmann,<sup>7</sup> C. A. Diget,<sup>8</sup> H. A. Falou,<sup>9</sup> B. R. Fulton,<sup>8</sup> H. O. U. Fynbo,<sup>10</sup> D. Galaviz,<sup>11</sup> J. Gómez-Camacho,<sup>1,2</sup> R. Kanungo,<sup>9</sup> J. A. Lay,<sup>1</sup> M. Madurga,<sup>3</sup> I. Martel,<sup>12</sup> A. M. Moro,<sup>1</sup> I. Mukha,<sup>1</sup> T. Nilsson,<sup>13</sup> A. M. Sánchez-Benítez,<sup>12</sup> A. Shottor,<sup>14</sup> O. Tengblad,<sup>3</sup> and P. Walden<sup>7</sup>

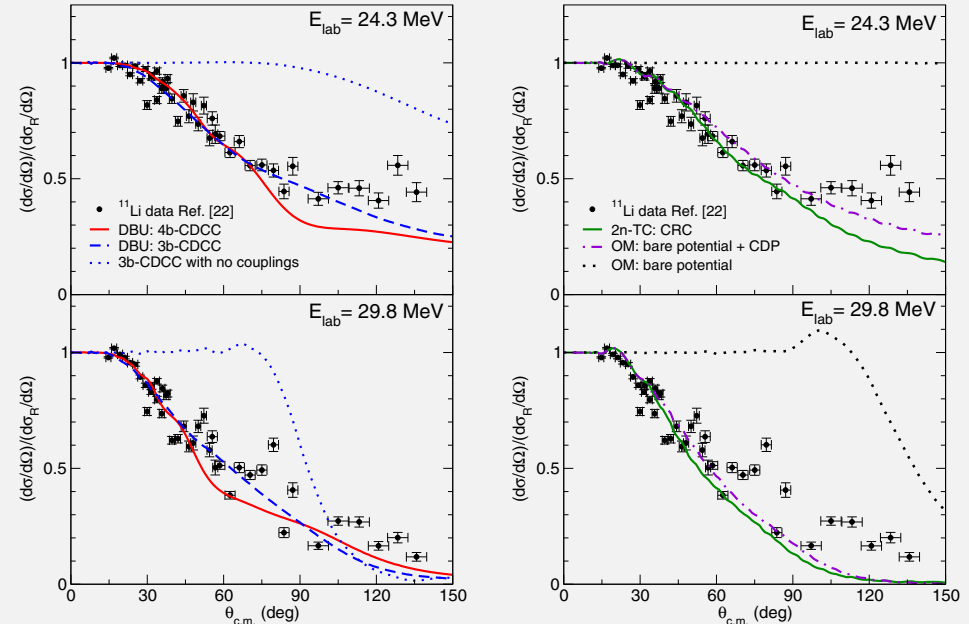
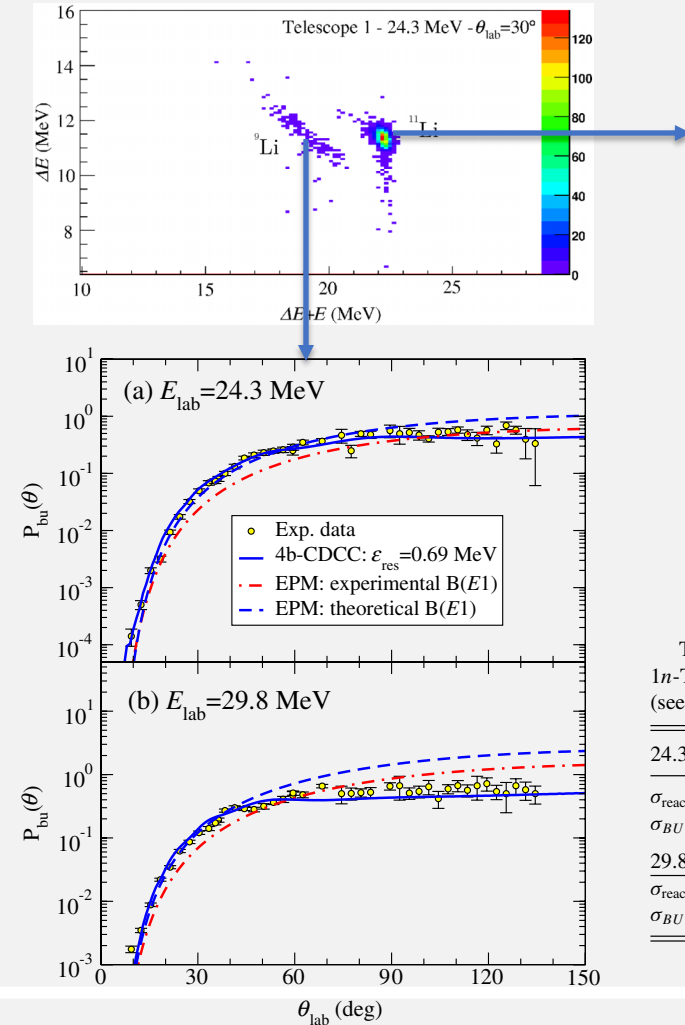
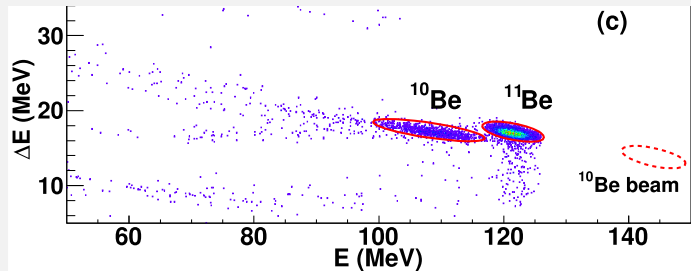


TABLE II. Comparison of the experimental total reaction cross section ( $\sigma_{\text{reac}}$ ) and breakup cross section ( $\sigma_{\text{BU}}$ ) with the DBU, 2n-TC and 1n-TC mechanisms. The experimental reaction cross sections are obtained from the optical model fit to the elastic differential cross sections (see text for details).

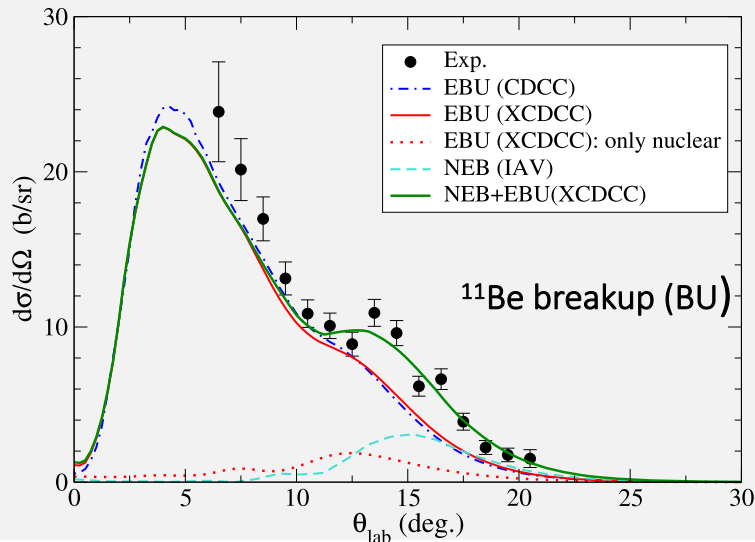
24.3 MeV	Exp. (mb)	DBU(4b-CDCC) (mb)	2n-TC (CRC) (mb)	1n-TC (CRC) (mb)
$\sigma_{\text{reac}}$	5400	6500	5500	5600
$\sigma_{\text{BU}}$	5100	4200	780	940
29.8 MeV	Exp. (mb)	DBU(4b-CDCC) (mb)	2n-TC (CRC) (mb)	1n-TC (CRC) (mb)
$\sigma_{\text{reac}}$	7800	8400	7100	7900
$\sigma_{\text{BU}}$	6500	5400	1100	1000

# $^{11}\text{Be} + ^{208}\text{Pb}$ breakup @ 140 MeV

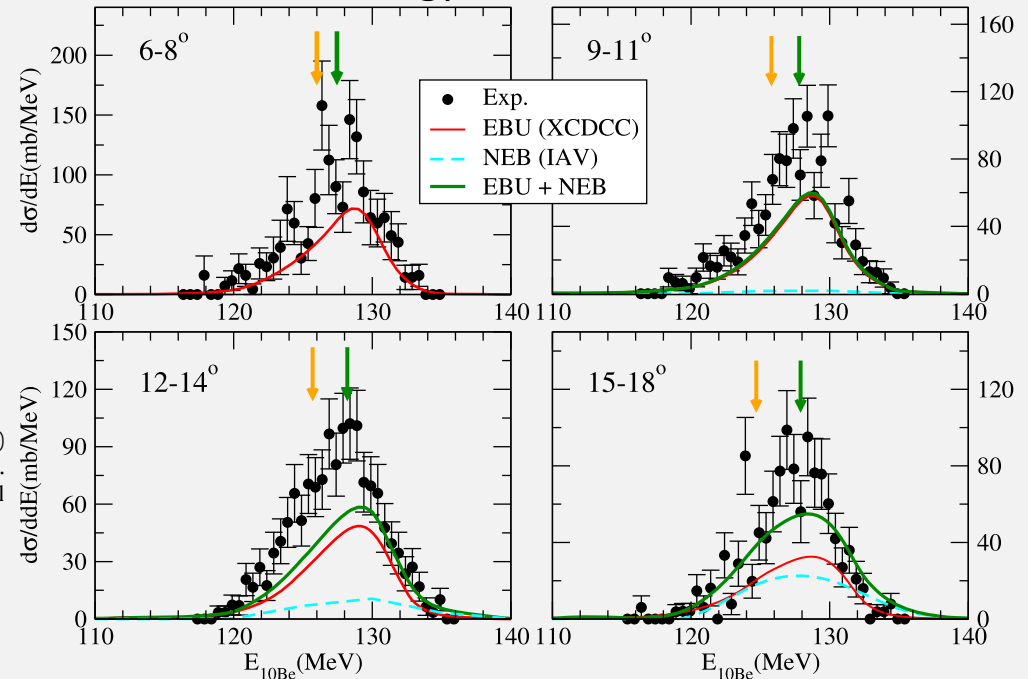


**Fig. 2.** The two-dimensional  $\Delta E - E$  particle identification spectra for the (a)  $^9\text{Be}$ , (b)  $^{10}\text{Be}$  and (c)  $^{11}\text{Be}$  beams within all the angles covered by the current measurement. In (c), the expected loci of  $^{10}\text{Be}$  beam contamination are indicated and it is well separated from the group of  $^{10}\text{Be}$  breakup fragment particles.

## $^{10}\text{Be}$ angular distribution



## $^{10}\text{Be}$ energy distribution



Scattering of the halo nucleus  $^{11}\text{Be}$  from a lead target at 3.5 times the Coulomb barrier energy

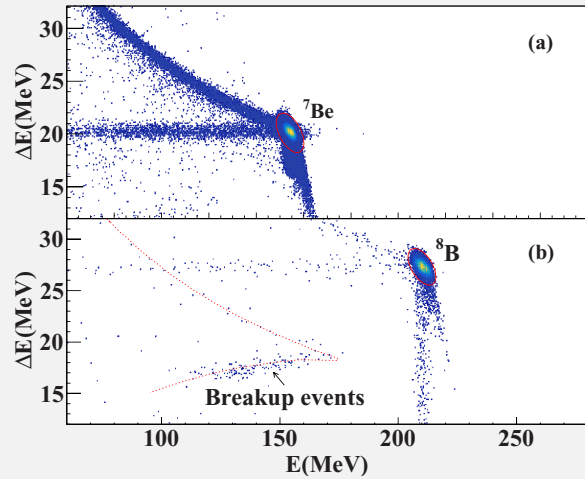
RIBLL Collaboration

F.F. Duan<sup>a,b,1</sup>, Y.Y. Yang<sup>a,c,e,\*,1</sup>, K. Wang<sup>a</sup>, A.M. Moro<sup>d,e,\*,1</sup>, V. Guimarães<sup>f</sup>, D.Y. Pang<sup>g</sup>, J.S. Wang<sup>h,a,c</sup>, Z.Y. Sun<sup>a,c</sup>, Jin Lei<sup>a,2</sup>, A. Di Pietro<sup>1</sup>, X. Liu<sup>1</sup>, G. Yang<sup>a,c</sup>, J.B. Ma<sup>a,c</sup>, P. Ma<sup>a</sup>, S.W. Xu<sup>a</sup>, Z. Bai<sup>a</sup>, X.X. Sun<sup>a</sup>, Q. Hu<sup>a</sup>, J.L. Lou<sup>a</sup>, X.X. Xu<sup>a,c</sup>, H.X. Li<sup>a</sup>, S.Y. Jin<sup>a</sup>, H.J. Ong<sup>a</sup>, Q. Liu<sup>1</sup>, J.S. Yao<sup>h</sup>, H.K. Qi<sup>h</sup>, C.J. Lin<sup>h</sup>, H.M. Jia<sup>h</sup>, N.R. Ma<sup>h</sup>, L.J. Sun<sup>m,n</sup>, D.X. Wang<sup>m</sup>, Y.H. Zhang<sup>a,c</sup>, X.H. Zhou<sup>a,c</sup>, Z.G. Hu<sup>a,c</sup>, H.S. Xu<sup>a,c</sup>

Total Bu cross-section  $\sim 3632$  mb

Total reaction cross sections is 7798 mb  $^{11}\text{Be}$ .



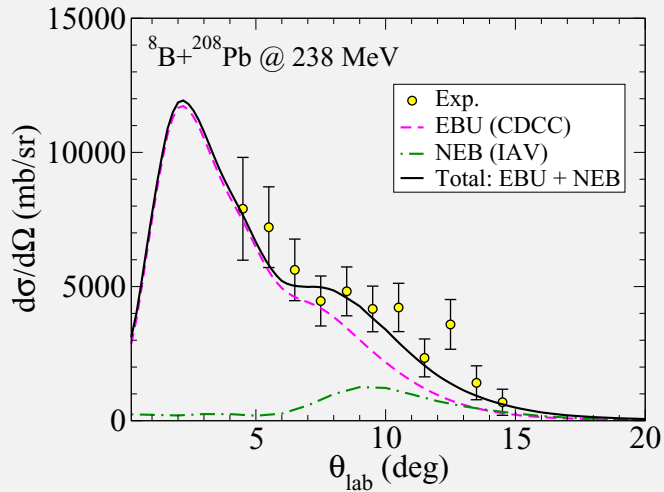
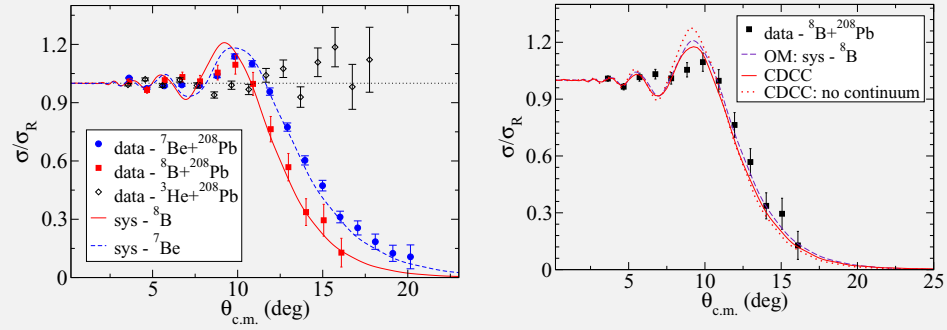


### Elastic scattering and breakup reactions of the proton drip-line nucleus $^8\text{B}$ on $^{208}\text{Pb}$ at 238 MeV

K. Wang,<sup>1</sup> Y. Y. Yang,<sup>1,2,\*</sup> A. M. Moro,<sup>3,4</sup> V. Guimarães,<sup>5</sup> Jin Lei,<sup>6</sup> D. Y. Pang,<sup>7</sup> F. F. Duan,<sup>1</sup> J. L. Lou,<sup>8</sup> J. C. Zamora,<sup>5</sup> J. S. Wang,<sup>9,1,2</sup> Z. Y. Sun,<sup>1</sup> H. J. Ong,<sup>1,2,10</sup> X. Liu,<sup>11</sup> S. W. Xu,<sup>1</sup> J. B. Ma,<sup>1</sup> P. Ma,<sup>1</sup> Z. Bai,<sup>1</sup> Q. Hu,<sup>1</sup> X. X. Xu,<sup>1,2</sup> Z. H. Gao,<sup>1</sup> G. Yang,<sup>1,2</sup> S. Y. Jin,<sup>1,2</sup> Y. H. Zhang,<sup>1,2</sup> X. H. Zhou,<sup>1,2</sup> Z. G. Hu,<sup>1,2</sup> and H. S. Xu<sup>1,2</sup>  
(RIBLL Collaboration)

K. WANG *et al.*

PHYSICAL REVIEW C **103**, 024606 (2021)



dominance of EBU @ 238 MeV

779 mb BU cross-section

Total reaction CS = 3423 mb

FIG. 5. Experimental  $^7\text{Be}$  angular distributions from the  $^8\text{B} + ^{208}\text{Pb}$  reaction at  $E_{lab} = 238$  MeV (yellow circle) and comparisons with calculations. Error bars are statistical only.

## Conclusions:

- The fragments energy and angular distributions in  $^8\text{Li}$  reactions indicate that the dominant process at low energies is the neutron transfer/non-elastic breakup (NEB) rather than elastic breakup. Elastic breakup seems to give a minor contribution at low energies.
- The transferred particle (neutron) interacts strongly with the target, exciting the recoil system over a wide excitation energy range from bound to unbound states with a maximum cross-section below the neutron threshold. The fragments energy distributions are well described by IAV calculations and momentum matching conditions as predicted by Q-optimum calculations.
- The coupling between the transfer and the elastic channels explain the backward rise observed in the  $^8\text{Li}$ +target elastic scattering angular distributions.
- For  $^6\text{He}$  projectiles, it seems that there is a transition from transfer (or NEB) to elastic breakup as the beam energy increases.
- The total breakup cross section increases relatively to the total reaction cross section for lower energies, in some cases, reaching almost 100% of the total reaction cross section.

*Universidade de São Paulo, IFUSP*

R. Lichtenthäler Fº, K.C.C. Pires, O.C. B. Santos, U.U. da Silva, A. Serra, B. Penteado Monteiro, H. F. Gonçalves de Arruda, K. Albuquerque, G. S. Gonçalves, H. A. Cabral Teixeira, I. Rojahn da Silva, M. V. Rodrigues Ribeiro, H. C. Sarambeli, S. Appannababu, J. Zamora, E. Zevallos, K Grupett, V.Guimarães, A. Lépine-Szily,

*IFUSP-J.R. Brandão de Oliveira*

*Universidad de Sevilla, Espanha*

M. Rodríguez-Gallardo, A.M. Moro

*University of Notre Dame, USA*

J. Kolata, F. Becchetti

*Université Libre de Bruxelles*

P. Descouvemont

*IEA-USP*

M. S. Hussein

*Laboratorio Tandem, Buenos Aires, Argentina*

A. Arazi

*CEADEN, Havana, Cuba*

I.Padron, J. Arteché, R. Arteché

*Instituto de Pesquisas Energeticas e Nucleares (IPEN)*

J.M.B. Shorto

*Universidade Federal Fluminense (UFF)*

P.R.S. Gomes, J. Lubian, R. Linares, P. N. de Faria, D. R. Mendes, M.C. Morais

*Universidade Federal de São Paulo (UNIFESP)*

M. Assunção

*Universidade Federal Rural do Rio de Janeiro (UFRRJ)*

V. Morcelle

*Universidade Federal de São Paulo (UNIFESP)*

A. Barioni

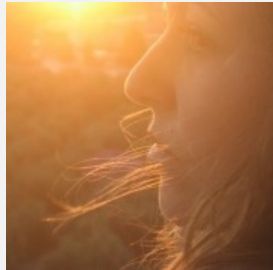
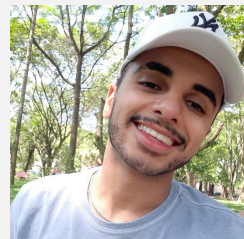
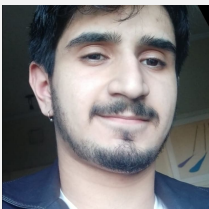
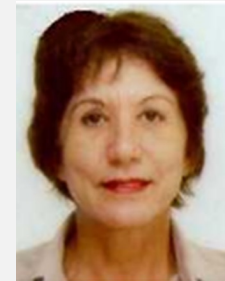
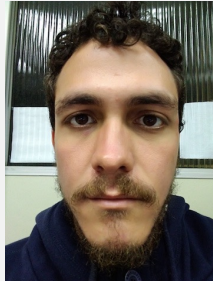
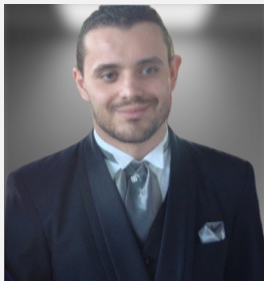
## PRESENT RIBRAS TEAM

PROFS: R. Lichtenthäler F<sup>o</sup>, K.C.C. Pires, A. Lépine (Senior).

Pós-docs: O.C. B. Santos, U.U. da Silva, A. Serra, O. Sunday Daniel.

Master/Phd: B. Penteado Monteiro, H. F. Gonçalves de Arruda.

Iniciação científica: , H. A. Cabral Teixeira, G. S. Gonçalves, K. Albuquerque, I. Rojahn da Silva, M. V. Rodrigues Ribeiro, H. C. Sarambeli.



Collaborators from Sevilla group

Antônio Moro

Manuela Rodríguez-Gallardo

and José Roberto Brandão de Oliveira from IFUSP

Thank you!